Composite and Cascaded Generalized-K Fading Channel Modeling and Their Diversity and Performance Analyses

Thesis by

Imran Shafique Ansari, B.Sc.

Submitted in Partial Fulfillment of the Requirements for the degree of

Masters of Science

King Abdullah University of Science and Technology

Division of Physical Sciences and Engineering

Electrical Engineering Program

Thuwal, Makkah Province, Kingdom of Saudi Arabia

December, 2010

The undersigned approve the thesis of Imran Shafique Ansari

Dr. Basem Shihada   Signature   Date
Committee Member

Dr. Saad Al-Ahmadi   Signature   Date
Committee Member

Dr. Mohamed-Slim Alouini   Signature   Date
Committee Chair(Thesis Supervisor)

King Abdullah University of Science and Technology

2010

ABSTRACT

Composite and Cascaded Generalized-K Fading Channel

Modeling and Their Diversity and Performance Analyses

Imran Shafique Ansari

The introduction of new schemes that are based on the communication among nodes has motivated the use of composite fading models due to the fact that the nodes experience different multipath fading and shadowing statistics, which subsequently determines the required statistics for the performance analysis of different transceivers.

The end-to-end signal-to-noise-ratio (SNR) statistics plays an essential role in the determination of the performance of cascaded digital communication systems. In this thesis, a closed-form expression for the probability density function (PDF) of the end-end SNR for independent but not necessarily identically distributed (i.n.i.d.) cascaded generalized-K (GK) composite fading channels is derived. The developed PDF expression in terms of the Meijer-G function allows the derivation of subsequent performance metrics, applicable to different modulation schemes, including outage probability, bit error rate for coherent as well as non-coherent systems, and average channel capacity that provides insights into the performance of a digital communication system operating in N cascaded GK composite fading environment.

Another line of research that was motivated by the introduction of composite fading channels is the error performance. Error performance is one of the main performance measures and derivation of its closed-form expression has proved to be quite involved for certain systems. Hence, in this thesis, a unified closed-form expression, applicable to different binary modulation schemes, for the bit error rate of dual-branch selection diversity based systems undergoing i.n.i.d. GK fading is derived in terms of the extended generalized bivariate Meijer G-function.

Acknowledgments

I would like to sincerely thank my supervisor Dr. Mohamed-Slim Alouini for his continuous guidance and encouragement throughout the course of this work. His enthusiasm and valuable feedback for research made my study very enjoyable and exciting and ultimately fruitful with rich experience. I would also like to thank him for providing me with an amazing research environment.

I would also like to thank Dr. Halim Yanikomeroglu, Carleton University for his enormous support during this journey with unlimited encouragement. He hosted me for summer internship during Summer 2010 and since then has never stepped back in assisting me in all aspects of life.

I would also like to thank Dr. Ferkan Yilmaz, King Abdullah University of Science and Technology (KAUST) and Dr. Saad Al-Ahmadi, Carleton University for their great technical support. They have been there to support me in almost every hurdle during this journey and encourage and motivate me to get the work done with excellence and ahead of time.

I thank my parents for their continuous encouragement and my siblings for bearing with me for my negligence towards them during this journey and their deep moral support at all times.

Additionally, I would like to thank Dr. Alouini's research group members i.e. the inhabitants of Building 1, Level 3, 3139 area cubicles for making the environment very research friendly and exciting to work.

Lastly, I would like to thank the people at KAUST, Thuwal, Makkah Province, Saudi Arabia, and Carleton University, Ottawa, Canada for providing support and resources, respectively for this research work.

TABLE OF CONTENTS

List of Figures

List of Tables

NOMENCLATURE

ACRONYMS

Symbol	Meaning
AF	Amount of fading
AWGN	Additive White Gaussian Noise
BER	Bit error rate
BPSK	Binary phase shift keying
BFSK	Binary frequency shift keying
CDF	Cumulative density function
CEP	Conditional error probability
CF	Characteristic function
CSI	Channel state information
DPSK	Differential phase shift keying
EC	Ergodic capacity
EGBMGF	Extended generalized bivariate Meijer G-function
EGC	Equal-gain combining
GK	Generalized-K
GNM	Generalized Nakagami-m
i.n.i.d.	Independent and non-identically distributed
i.i.d.	Independent and identically distributed
LOS	Line of sight
NLOS	Non-line of sight
MGF	Moment generating function
MIMO	Multiple-input multiple-output
MISO	Multiple-input single-output
MRC	Maximal ratio combining
OP	Outage probability
PDF	Probability Density Function
RV	Random Variable
SC	Selection combining
SIMO	Single-input multiple-output
SISO	Single-input single-output
SNR	Signal-to-noise ratio
STBC	Space-time block code
TIMO	Two-input multiple-output

LIST OF SYMBOLS

Symbol	Meaning
C	Channel capacity
γ	Instantaneous power
$\Gamma(\cdot)$	Gamma function
${}_pF_q$	The generalized hypergeometric function for integers p and q
K_m	The modified Bessel function of second kind and order m
$H_{p,q}^{m,n}$	The Fox H-function with parameters m, n, p, and q
$G_{p,q}^{m,n}$	The Meijer G-function with parameters m, n, p, and q
$S[\cdot]$	The extended generalized bivariate Meijer G-function
$G_{p_1,q_1:p_2,q_2:p_3,q_3}^{m_1,n_1:m_2,n_2:m_3,n_3}$	The extended generalized bivariate Meijer G-function with parameters m_1, n_1, m_2, n_2, m_3, n_3, p_1, q_1, p_2, q_2, p_3, and q_3

Chapter I

Introduction

I.1   Wireless Channel Modeling and Composite Fading Channels

In wireless channels, a radiated electromagnetic wave interacts with the medium between the transmitter and the receiver in a complicated way i.e. the incident wave interacts with surface irregularities via diffraction, scattering, reflection, and absorption creating a chain or a flow of scattered partial waves. Besides this, the physical properties of the surface structure such as geometrical proportions and electromagnetic reflection properties also influence the amplitudes and phases of such type of partial waves. Hence, in space, such scattered partial waves interfere with each other and possibly with the direct wave, building up an irregular electromagnetic field. On the other hand, the signal power tends to decrease with distance and the existence of large scatterers such as trees, buildings, and mountains introduces random variations of the local mean of the envelope or equivalently the local mean power. Hence, global deterministic characterization is not possible and can only be specific. Therefore, the only way to characterize such channel is probabilistic. In other words, to statistically

model wireless channels, these small-scale and large-scale propagation mechanisms are to be considered independently [2].

Having mentioned small-scale fading above, it occurs due to the superposition of the received multipath signals which are due to the processes of reflection, diffraction, and scattering. Hence, within a scale that is comparable to the carrier wavelength, the superposition of the multipath signals may add constructively (in-phase) or destructively (out-of-phase) causing the phenomenon of small-scale fading or multipath fading.

Whereas, the scattering caused due to the presence of general terrain, large buildings and vegetation wherein the local mean received power varies in a wireless channel is a phenomenon that is referred to as large-scale fading or shadowing.

Additionally, wireless communications are driven by a complicated phenomenon known as radio-wave propagation that is characterized by various effects including multipath fading and shadowing. The statistical behavior of these effects is described by different models depending on the nature of the communication environment. It is becoming necessary to study such effects. Hence, we intend to study large-scale fading as well as small-scale fading concurrently as the multihop relay networks are emerging in the current times.

Now, since the geographically distributed nodes experience different multipath fading and shadowing statistics, hence, modeling composite fading channels, where the multipath fading and shadowing are modeled jointly, is essential for the performance analysis of different communication systems.

I.2   Cascaded Channels

The concept of using mobile terminals as relay stations is emerging as a feasible option for overcoming the problems of the next generation wireless networks. Conventional

relaying systems use relays as pure forwarders whereas cooperative relays tackle the fundamental features of wireless medium i.e. its broadcast nature, and its ability to provide independent channels and hence achieving diversity. Cooperative networks benefit from the broadcast nature because of the fact that once a signal is transmitted, it can be received and usefully forwarded by multiple terminals [3].

Nevertheless, whichever type of relaying system one employs, it encompasses the concept of multiple scattering radio propagation channels [4] that has been proved useful in many scientific fields of communications and to fit many propagation scenarios in the recent past. For instance, in a multihop communication system [5], the source node communicates with the destination node via a given number of N hops. Those intermediate nodes called hops are analog repeaters i.e. operate under amplify-and-forward relay with fixed gains and hence, such a channel accounts to a cascaded channel that can be modeled as a product of fading amplitudes or this can also be referred to as multiplicative fading models.

In other words, wireless multihop transmission exploits wireless cascaded channel wherein each relay terminal multiplies the received signal from the previous terminal by a constant gain determined by path-loss without performing phase-correction. This forms an efficient technology for extending the coverage with respect to the channel path-loss and increasing the channel capacity of wireless communications especially in severe multipath fading channels [1].

Hence, these so-called cascaded fading channels have recently gained significant interest in modeling the propagation environment. These models can be physically interpreted by considering received signals generated by the product of a large number of rays reflecting N statistically independent scatterers. This concept of cascaded channels is analogous to modeling propagation via keyholes [6] or via diffracting wedges like rooftops or street corners, among others [4], as shown below in figure I.1. The γ_n's in the figure represent the channel model.
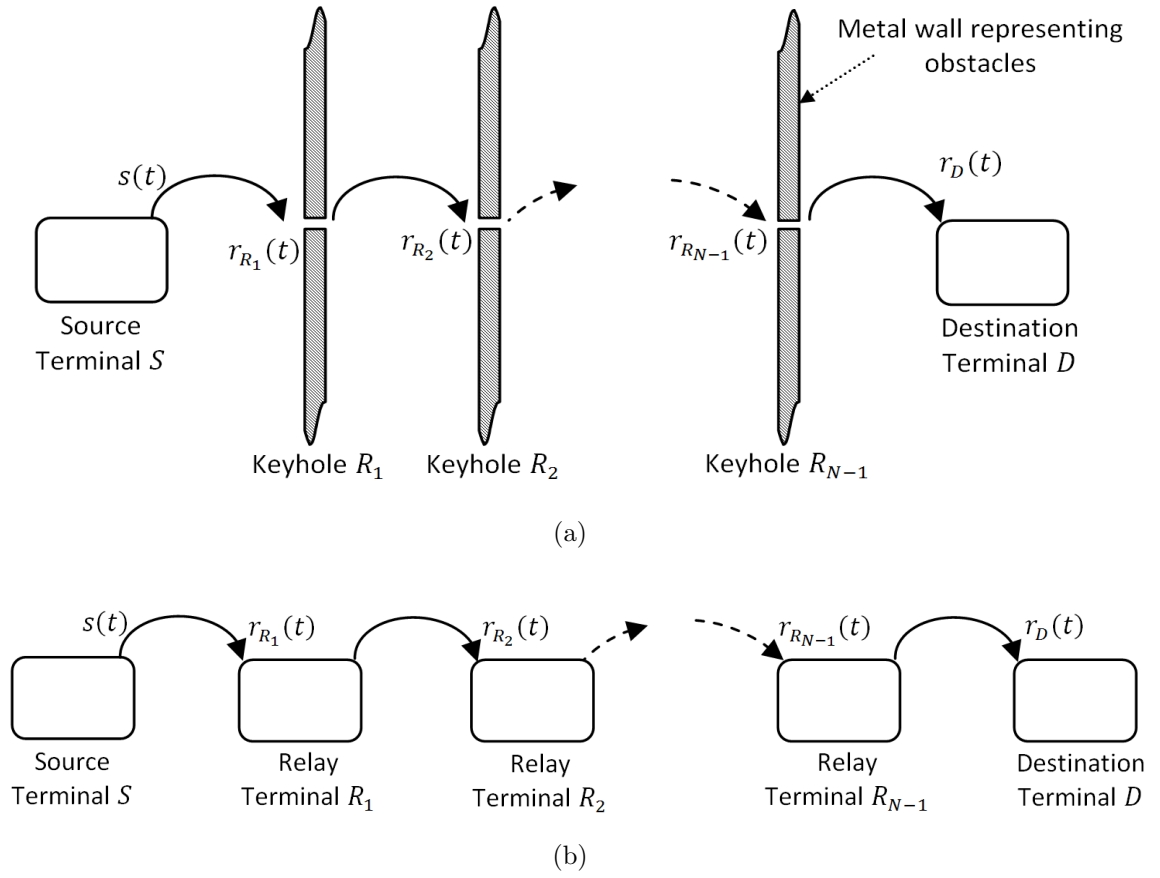
Figure I.1: Propagation scenarios of cascaded fading channels: (a) cascaded fading channels created by keyholes, (b) cascaded fading channels created by amplify-and-relay terminals [1].

This can be physically interpreted by considering a source and a destination terminal surrounded by several stationary and moving objects such that the signal transmitted by the source terminal can propagate to the receiver only through minute apertures (that can be considered as keyholes), among obstacles. Hence, each such keyhole then acts as a source terminal to the next keyhole thus forming the complete communication channel that can be considered as a cascaded fading channel [7].

Cascaded fading models have proved to be useful in the performance analysis of space-time block codes (STBCs) over different channel models. Additionally, they have also proved useful in analytical study of the performance of equal-gain combining (EGC) diversity receivers [7].

Besides having a discussion of cascaded channels wherein there are relays connected in series forming a chain, its worthwhile to discuss the possibility of having these relays connected between the source node and the destination node in a parallel fashion leading to multiple copies of same message reaching at the receivers end. This parallel fashion allows employment of different types of schemes to achieve better system performance. Following section discusses this concept further.

I.3 Selection Diversity

In wireless systems with base stations or access points communicating with small low power terminals, the terminals may be limited to a single transmit chain due to power complexity constraints. On the contrary, multiple transmit and receive antenna systems i.e. multiple input and multiple output (MIMO) systems offer substantial performance improvement in wireless systems by increasing their spectral efficiency and/or by reducing the effects of the channel impairments [8].

One of the most simplest and most efficient techniques to overcome the destructive effects of fading in wireless communication systems, as of yet, is diversity. In all

of these diversity techniques, the receiver processes the obtained diversity signals in a way that maximizes the system's power efficiency. There are several diversity techniques such as EGC, maximal ratio combining (MRC), selection combining (SC), and a combination of MRC and SC referred to as generalized selection combining (GSC). Intuitively and also it is a proved fact that among these diversity techniques, SC is the least complicated. This is because the processing is done only on one of the diversity branches of the receiver [9]. Hence, diversity reception can significantly improve the performance of wireless communication systems in the presence of multipath fading and interference [10].

Recently, there has been considerable interest in low-complexity combining schemes for diversity-rich environments. Diversity combining is one of the most effective fading-mitigation techniques. In general, the performance of wireless communication systems improves as the number of available diversity paths increases. Therefore, emerging wireless communication systems are employing physical-layer solutions operating in diversity-rich environments, or in other words, with a larger number of diversity paths. For instance, ultra-wideband code-division multiple-access systems, millimeter-wave systems and MIMO systems [11].

Additionally, different diversity schemes have taken up an important role in wireless communication systems. The main reason behind this is that these different diversity schemes allow for multiple transmission and/or reception paths for the same signal [12]. One of the simplest diversity combining scheme, as mentioned above, is the SC diversity scheme where only one of the diversity branches is processed. Specifically, SC scheme chooses the branch with highest signal-to-noise ratio (SNR) that corresponds to the strongest signal if equal power is assumed among the different branches [13]-[14]. Therefore, for simplicity, this SC scheme has been employed in the current work and the positive results encourage to further work on different diversity techniques.

I.4 Objectives and Contributions

The main objective of this thesis is to contribute toward appropriate channel modeling, cascaded channels, and dual SC under generalized-K (GK) fading environment where the GK model is described in the upcoming chapter.

A very essential tool for performance analysis of wireless communication systems is the underlying composite fading model where the effects of both multipath fading and shadowing are incorporated. Hence in Chapter II, an introductory background to a simple yet sufficiently accurate composite fading model i.e. the GK fading model that bypasses the analytical and numerical difficulties associated with the existing models in literature is presented. Further, some statistical characteristics of the GK model including its probability density function (PDF) and cumulative density function (CDF) are discussed.

In Chapter III, a closed-form expression of the PDF of the end-end SNR for independent but not necessarily identically distributed (i.n.i.d.) cascaded GK composite fading channels is derived. The developed PDF expression in terms of the Meijer-G function (refer Appendix A) allows the derivation of subsequent performance metrics, applicable to different modulation schemes, including outage probability (OP), bit error rate (BER) for coherent as well as non-coherent systems, and average channel capacity (EC) that provides insights into the performance of a digital communication system operating in N cascaded GK composite fading environment.

Using the results obtained in Chapter II, a unified closed-form expression, applicable to different binary modulation schemes, for the BER of dual-branch diversity SC based systems undergoing i.n.i.d. GK fading is derived in terms of the extended generalized bivariate Meijer G-function (EGBMGF) in Chapter IV.

The contributions of this thesis folds in the following streams:

- The discussion of the GK model and presenting some of its statistical characteristics including its PDF and CDF. The important outcome to be taken into

consideration is the derivation of CDF i.e. it has been derived directly from the PDF rather than employing the relatively complex moment generating function (MGF) approach.

- The derivation of the PDF expression and various performance metrics for a cascaded system running under GK environment.

- Derivation of the exact closed-form BER expression for a dual-branch diversity SC system running under GK environment.

Chapter II

The Generalized-K Fading System and Channel Model

Considering the case wherein we have shadowing in addition to the multipath fading considered previously, each receiver is subject to a composite fading signal [12]. For such a scenario, several composite fading models have been proposed such as Suzuki [15], Nakagami-lognormal [16], Rice-lognormal [17] and Generalized-K (GK) [18] etc. Unfortunately for the first three models, closed form probability density function (PDF) does not exists making further performance analysis difficult. With regards to the latter model, acknowledging their contribution, the authors in [7] and [19] have proposed a statistical characterization of GK model via deployment of a rather complicated moment generating function (MGF) approach.

Using the Nakagami multipath fading model that is versatile enough to model various multipath fading conditions ranging from severe fading to non-fading scenario, and the Gamma model for shadowing [20], has led to the GK (Gamma-Gamma) composite fading model [18], [21]-[24]. GK distribution, earlier used in radar applications and recently being used in the context of wireless digital communications over fading channels, is one of the relatively new tractable models used to describe the statistical

behavior of multipath fading and shadowing effects as compared to log-normal based models. As an instance to the above statement, the desired relationship between the parameter of Gamma PDF and the log-normal PDF is given by [23] as

$$m_s = \frac{1}{\exp(\sigma^2) - 1}. \tag{II.1}$$

Furthermore, GK fading model is quite general model as it includes K-distribution [25] as its special case and accurately approximates many other fading models such as Nakagami-m and Rayleigh-Lognormal (R-L) ([22] and references therein). Finally, GK distribution is a distribution of the product of two independent Gamma random variables (RV) and hence is a special case of the Fox H-function (refer Appendix A) and in turn a special case of Meijer G-function where the product of two Meijer G-function's can be represented in terms of the extended generalized bivariate Meijer G-function (EGBMGF) (refer Appendix B) [26].

II.1   Basic Model

A multi-hop communication system with a source, a destination, and (N-1) intermediate relay nodes is considered. The channel gain for the nth hop is denoted by h_n. In a Nakagami multipath fading channel, $\gamma = |h_n|^2$ follows Gamma distribution; additionally, the shadowing component is also assumed to follow a Gamma distribution. Hence, the channel gains experience composite fading whose statistics follow a GK distribution given by

$$p_\gamma(\gamma) = \frac{2b^{m_m+m_s}}{\Gamma(m_m)\Gamma(m_s)}\gamma^{\frac{m_m+m_s}{2}-1}K_{m_s-m_m}(2b\sqrt{\gamma}), \gamma > 0, \tag{II.2}$$

where $\Gamma(\cdot)$ is the Gamma function as defined in [27, Eq. (8.310)], m_m and m_s are the Nakagami multipath fading and shadowing parameters, respectively. In (II.2) $K_m(\cdot)$

is the modified Bessel function of the second kind and order m, $b = \sqrt{\frac{m_m m_s}{\Omega_0}}$, and Ω_0 is the mean of the local power. The parameters m_m and m_s quantify the severity of multipath fading and shadowing, respectively, in the sense that small values of m_m and m_s indicate severe multipath fading and shadowing conditions respectively, and vice versa. Additionally, $m_m = 1$ represents the non-line of sight (NLOS) branch and $m_m = 2$ represents the line of sight (LOS) branch. The instantaneous signal-to-noise ratio (SNR) of the nth branch/relay is given by $\gamma_n = (E_b/N_0) x_n^2$ where x_n is the signal amplitude for the nth branch, E_b is the average energy per bit and N_0 is the power spectral density (PSD) of the additive white Gaussian noise (AWGN).

II.2   Statistical Characteristics

The PDF and cumulative density function (CDF) expressions of the GK RVs can also be written in terms of Meijer G-function. This section presents some interesting and very useful characteristics of GK fading channel.

Lemma 1: The PDF of a GK RV can be expressed in terms of the Meijer-G function as

$$p_\gamma(y) = \left(\frac{m_m m_s}{\Gamma(m_m)\,\Gamma(m_s)\,\Omega_0}\right) G_{0,2}^{2,0}\left[\left(\frac{m_m m_s}{\Omega_0}\right)y \,\middle|\, m_m - 1, m_s - 1\right], y > 0. \quad \text{(II.3)}$$

Proof. We may use the fact that the PDF of the product of N independent Gamma RVs can expressed as a H-function PDF that is given by [28, Eq. (6.4.9)] as follows

$$p(x) = \left(\prod_{i=1}^{N} \frac{1}{\theta_i \Gamma(k_i)}\right) H_{0,N}^{N,0}\left[\left(\prod_{1}^{N} \frac{1}{\theta_i}\right)x \,\middle|\, (k_i - 1, 1), \ldots, (k_N - 1, 1)\right], x > 0. \quad \text{(II.4)}$$

Then, with $N = 2$, the GK PDF can be expressed as

$$p(x) = \left(\frac{m_m m_s}{\Gamma\left(m_m\right)\Gamma\left(m_s\right)\Omega_0} \right) H_{0,2}^{2,0} \left[\left(\frac{m_m m_s}{\Omega_0} \right) x \,\middle|\, \left(m_m - 1, 1\right), \left(m_s - 1, 1\right) \right], x > 0.$$

(II.5)

Now by applying [28, Eq. (6.2.8)], the expression in (II.3) follows. □

Further, substituting (II.3) in [29, Eq. (26)] and utilizing [28, Eq. (6.2.4)], the CDF of GK can be written as

$$P_\gamma(\gamma) = \frac{1}{\Gamma\left(m_m\right)\Gamma\left(m_s\right)} G_{1,3}^{2,1} \left[\left(\frac{m_m m_s}{\Omega_0} \right) \gamma \,\middle|\, \begin{matrix} 1 \\ m_m, m_s, 0 \end{matrix} \right], \gamma > 0,$$

(II.6)

where $G[\cdot]$ is the Meijer G-function [27].

Chapter III

Exact SNR Statistics for Cascaded Generalized-K Composite Fading Channels

Modeling of composite fading channels, where the multipath fading and shadowing effects are incorporated, is essential for analyzing the performance of different communication schemes. In this chapter, an overview of the current models of multipath fading and shadowing is first given and the generalized-K(GK) composite fading model is then presented. Secondly, signal-to-noise ratio (SNR) statistics for the cascaded GK composite fading channels is presented along with some performance metrics, including outage probability (OP), bit error rate (BER), and ergodic capacity (EC).

III.1 Related Work

Cascaded channels i.e. product of random variables (RVs) has been addressed quite extensively by the researchers in the near past from many different perspectives. As far as digital communication systems are concerned, the case of having propagation

with only multipath fading, related work includes performance analysis of cascaded Rayleigh [30], cascaded Nakagami-m [31] and cascaded Weibull channels [32]. Recently, cascaded channel modeling of multiple-input multiple-output (MIMO) systems has been used for the double Rayleigh model [6, 33] and the double Nakagami-m model [34]. Additionally, the product of Nakagami-m and Weibull RVs has found implementations in the performance of multihop relay networks [35, 36] and in the derivation of closed-form upper bounds for the distribution of the sum of RVs [37].

Considering the case where shadowing and multipath fading are considered, each receiver is subject to a composite fading signal [12]. For such a scenario, as mentioned in Chapter II, several composite fading models have been proposed such as Suzuki [15], Nakagami-lognormal [16], Rice-lognormal [17] and Generalized-K (GK) [18]. As discussed in Chapter II, unfortunately for the former three models, closed form probability density function (PDF) does not exists and hence halting further performance analysis whereas with regards to the later model, acknowledging their contribution, the authors in [7] and [19] have proposed a statistical characterization of GK model via deployment of a rather complicated moment generating function (MGF) approach. Similar work, with similar approach mentioned above, has been addressed for generalized Nakagami-m (GNM) [1].

In this chapter, the problem of independent but not necessarily identically distributed (i.n.i.d.) cascaded fading channels for GK fading environment with a PDF-based approach is addressed. In particular, the umbrella of the Meijer-G [27] function has been extensively used for the computation of the end-to-end SNR and complete further analysis. In addition, being aware of the flexibility of the GK model, the performance analysis including the computation of the OP, BER for both coherent as well as non-coherent modulation schemes and the average channel capacity or equivalently EC has been presented.

In th following section, we derive the computation of the end-to-end SNR of the

cascaded GK model followed by the performance analysis for the different performance metrics mentioned earlier.

III.2 End-to-End SNR Statistic

The end-to-end SNR in a non-regenerative (amplify-and-forward) multihop network, while considering a cascaded system or in other words having the intermediate nodes as keyholes as shown in earlier chapter in figure I.1, can be expressed as

$$\gamma = \prod_{n=1}^{N} \gamma_n, \tag{III.1}$$

where $\gamma_n = |h_n|^2$ is the SNR of the nth hop and N is the total number of hops.

In the following, the closed-form expression of the PDF for the end-to-end SNR in i.n.i.d. GK channels is derived. The derivations are based on the H-function (refer Appendix A) distribution umbrella.

Proposition: The PDF of the end-to-end SNR, as given in (III.1), can be expressed as

$$p(y) = \prod_{n=1}^{N} \left(\frac{m_{m_n} m_{s_n}}{\Gamma(m_{m_n}) \Gamma(m_{s_n}) \Omega_{0_n}} \right) G_{0,2N}^{2N,0} \left[\prod_{n=1}^{N} \left(\frac{m_{m_n} m_{s_n}}{\Omega_{0_n}} \right) y \middle| \kappa_1 \right], y > 0, \tag{III.2}$$

where $\kappa_1 = (m_{m_1} - 1), (m_{s_1} - 1), \ldots, (m_{m_N} - 1), (m_{s_N} - 1)$.

Proof. The proof is based on the representation of the GK PDF as H-function PDF and hence, subsequently utilizing the Lemma 1 presented in the previous chapter and [28, Theorem (6.4.1)], the PDF of γ can be expressed as

$$p(y) = \prod_{n=1}^{N} \left(\frac{m_{m_n} m_{s_n}}{\Gamma(m_{m_n}) \Gamma(m_{s_n}) \Omega_{0_n}} \right) H_{0,2N}^{2N,0} \left[\prod_{n=1}^{N} \left(\frac{m_{m_n} m_{s_n}}{\Omega_{0_n}} \right) y \middle| \kappa_2 \right], y > 0, \tag{III.3}$$

15

where $\kappa_2 = (m_{m_1} - 1, 1), (m_{s_1} - 1, 1), \ldots, (m_{m_N} - 1, 1), (m_{s_N} - 1, 1)$. This final expression can be written in a simplified Meijer G-function form using [28, Eq. (6.2.8)] as in (III.2).

$\square$

III.3   Performance Analysis

In this section, the developed expression for the end-end SNR is utilized to derive closed-form expressions for the different performance metrics such as OP, BER for both coherent and non-coherent modulation schemes and EC for a digital system operating over N i.n.i.d. cascaded GK composite fading channels.

III.3.1   Outage Probability

The outage probability P_{out} is defined as the percentage of time that the instantaneous SNR per symbol is below a certain threshold γ_{th} and can be expressed as

$$P_{out}(\gamma_{th}) = Pr\{\gamma \le \gamma_{th}\} = \int_0^{\gamma_{th}} p_\gamma(x)dx. \tag{III.4}$$

By using [29, Eq. (26)] (also refer Appendix C), P_{out} can be expressed in closed-form as

$$P_{out} = \text{CDF}(\gamma)|_{\gamma_{th}} = \left(\prod_{n=1}^N \frac{1}{\Gamma(m_m)\Gamma(m_s)}\right) G_{1,2N+1}^{2N,1}\left[\prod_{n=1}^N \left(\frac{m_{m_n}m_{s_n}}{\Omega_{0_n}}\right)\gamma_{th} \middle| \begin{matrix} 1 \\ \kappa_3, 0 \end{matrix}\right], \tag{III.5}$$

where $\kappa_3 = m_{m_1}, m_{s_1}, \ldots, m_{m_N}, m_{s_N}$.

III.3.2 BER Analysis

The average BER for the multihop relay networks is given by

$$P_b = \int_0^\infty P_e(\gamma) f_\gamma(\gamma) d\gamma. \tag{III.6}$$

Coherent Case

For coherent modulation schemes, the BER for the nonfading scenario can be expressed as

$$P_e(\gamma) = a \ \text{erfc}\left(\sqrt{b\gamma}\right), \tag{III.7}$$

and

$$\text{erfc}\left(\sqrt{b\gamma}\right) = \sqrt{\pi}^{-1} G_{1,2}^{2,0}\left[b\gamma \ \middle| \ \begin{matrix} 1 \\ 0, 1/2 \end{matrix}\right], \tag{III.8}$$

where a and b describe different modulation schemes. For example, for binary phase shift keying (BPSK), the corresponding values of are $a = 1/2$ and $b = 1$.

Now, substituting (III.2), (III.7) and (III.8) into (III.6) and using [27, Eq. (7.811)], we get

$$P_b = a\pi^{\frac{-1}{2}} \prod_{n=1}^{N} \left(\frac{m_{m_n} m_{s_n}}{\Gamma(m_{m_n}) \Gamma(m_{s_n}) \Omega_{0_n}}\right) \frac{1}{b} \ G_{2,2N+1}^{2N,2}\left[\frac{\prod_{n=1}^{N}\left(\frac{m_{m_n} m_{s_n}}{\Omega_{0_n}}\right)}{b} \ \middle| \ \begin{matrix} 0, -1/2 \\ \kappa_1, -1 \end{matrix}\right]. \tag{III.9}$$

Non-Coherent Case

For non-coherent modulation schemes, the BER for the nonfading scenario can be expressed as

$$P_e(\gamma) = c \ \exp(-d\gamma), \tag{III.10}$$

17

where c and d describe different modulation schemes. For example, for binary differential shift keying (DPSK), the corresponding values of are $c = 1/2$ and $d = 1$.

Now, substituting (III.2) and (III.10) into (III.6) and using [27, Eq. (7.813.1)] or [38], we get after some manipulations

$$P_b = c \prod_{n=1}^{N} \left(\frac{m_{m_n} m_{s_n}}{\Gamma(m_{m_n}) \Gamma(m_{s_n}) \Omega_{0_n}} \right) \frac{1}{d} \; G_{1,2N}^{2N,1} \left[\prod_{n=1}^{N} \left(\frac{m_{m_n} m_{s_n}}{\Omega_{0_n}} \right) \middle| \begin{array}{c} 0 \\ \kappa_1 \end{array} \right]. \qquad \text{(III.11)}$$

III.3.3 Ergodic Capacity

The ergodic capacity, assuming long coding periods over the composite fading realizations, is defined as

$$C = \int_0^\infty \log_2(1 + \gamma) f_\gamma(\gamma) d\gamma = \int_0^\infty \frac{\ln(1 + \gamma)}{\ln 2} f_\gamma(\gamma) d\gamma. \qquad \text{(III.12)}$$

Now using the fact that $\ln(1 + \gamma) = G_{2,2}^{1,2} \left[\gamma \middle| \begin{array}{c} 1, 1 \\ 1, 0 \end{array} \right]$ from [28, Eq. (6.4.2)] or [39], we may use [27, Eq. (7.811)] to express the ergodic capacity as

$$C = \frac{1}{\ln 2} \prod_{n=1}^{N} \left(\frac{m_{m_n} m_{s_n}}{\Gamma(m_{m_n}) \Gamma(m_{s_n}) \Omega_{o_n}} \right) G_{2,2N+2}^{2N+2,1} \left[\prod_{n=1}^{N} \left(\frac{m_{m_n} m_{s_n}}{\Omega_{0_n}} \right) \middle| \begin{array}{c} -1, 0 \\ -1, -1, \kappa_1 \end{array} \right].$$
$$\text{(III.13)}$$

III.4 Results and Discussions

The results for various performance metrics like OP, BER and EC for cascaded GK composite fading channels are presented in this section. Both, independent and identically distributed (i.i.d.) as well as i.n.i.d. channels are considered. The average SNR per bit in all the scenarios discussed is assumed to be equal. Additionally, in case of

BER, we have considered coherent BPSK (a=1/2 and b=1) and non-coherent DPSK (c=1/2 and d=1) systems. In Monte Carlo simulations, the GK fading channel was generated by the product of two independent gamma RVs.

In the following figures III.1 and III.2 we can observe that the developed expression in (III.1) for the end-to-end SNR of GK fading cascaded channels operating over varying hops ($N = 2, 3$, and 4) matches the Monte Carlo simulations perfectly for i.i.d. case as well as i.n.i.d. case respectively. The different values for multipath fading effect and shadowing effect for i.i.d. case were as follows; $m_m = 1$, and $m_s = 0.5$ whereas for i.n.i.d. case were $m_{m_1} = 0.5$, $m_{m_2} = 2$, $m_{m_3} = 1$, $m_{m_4} = 1$, $m_{s_1} = 0.5$, $m_{s_2} = 4$, $m_{s_3} = 2$, and $m_{s_4} = 10$. These values were selected randomly to prove the validity of the obtained results and hence specific values based on the standards can be used to obtain the required results. Similar outcomes can be observed for different number of hops i.e. different values of N and with other varying values for the multipath fading and shadowing parameters.
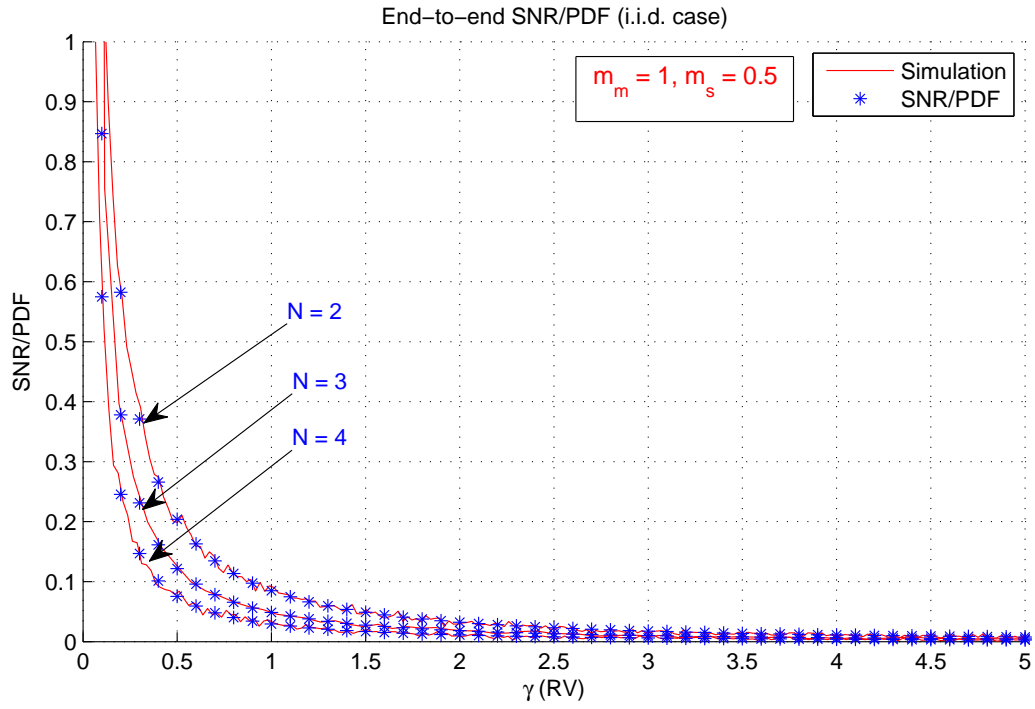
Figure III.1: End-to-end SNR/PDF for different (N) number of hops with i.i.d. channels having $m_m = 1$ and $m_s = 0.5$.
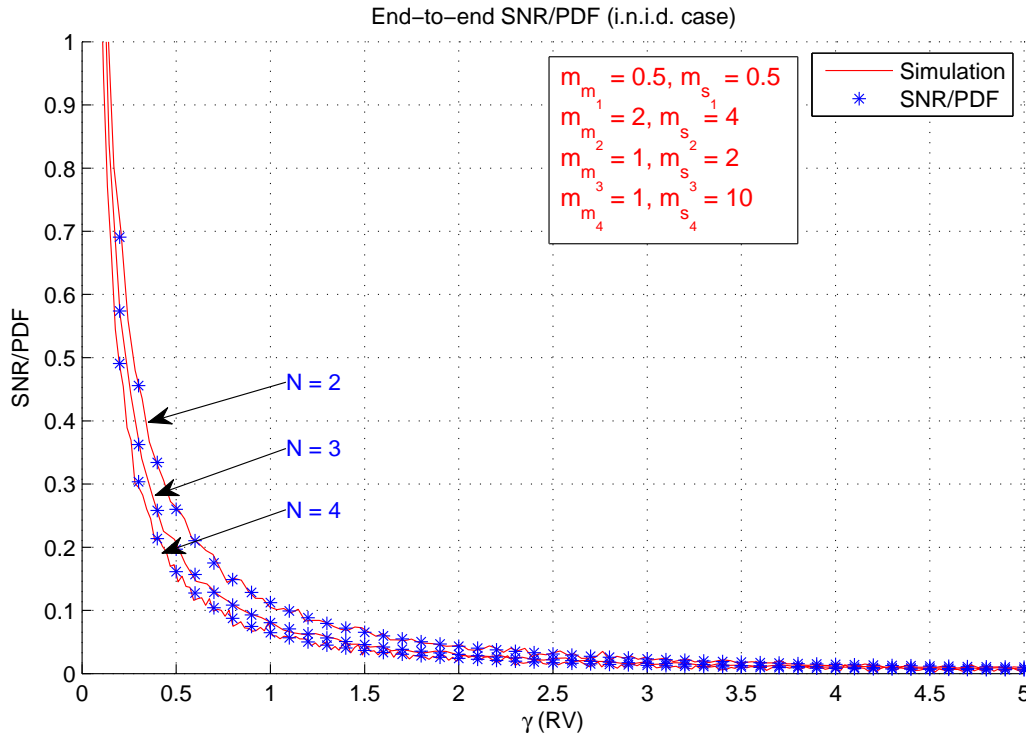
Figure III.2: End-to-end SNR/PDF for different (N) number of hops with i.n.i.d. channels having $m_{m_1} = 0.5$, $m_{m_2} = 2$, $m_{m_3} = 1$, $m_{m_4} = 1$, $m_{s_1} = 0.5$, $m_{s_2} = 4$, $m_{s_3} = 2$, and $m_{s_4} = 10$.

For comprehensive demonstration, from here onward, i.n.i.d. channels are considered and hence for i.i.d. case, similar Monte Carlo simulations will result into expected outcomes and in fact, it will be easier to simulate. The multipath fading and shadowing effect values employed are as $m_{m_1} = 2$, $m_{m_2} = 1$, $m_{m_3} = 0.5$, $m_{m_4} = 1$, $m_{s_1} = 1$, $m_{s_2} = 1.5$, $m_{s_3} = 4$, $m_{s_4} = 2$. These values were selected randomly to prove the validity of the obtained results and hence specific values based on the standards can be used to obtain the required results.

The derived expression in (III.5) matches with the Monte Carlo simulation shown figure III.3. The different specifications considered in the Monte Carlo simulations for OP were varying SNR from 0 dB through 20 dB, and a threshold of $\gamma_{th} = 0.001$. As expected, we see that as the number of hops N increases and as the SNR decreases,
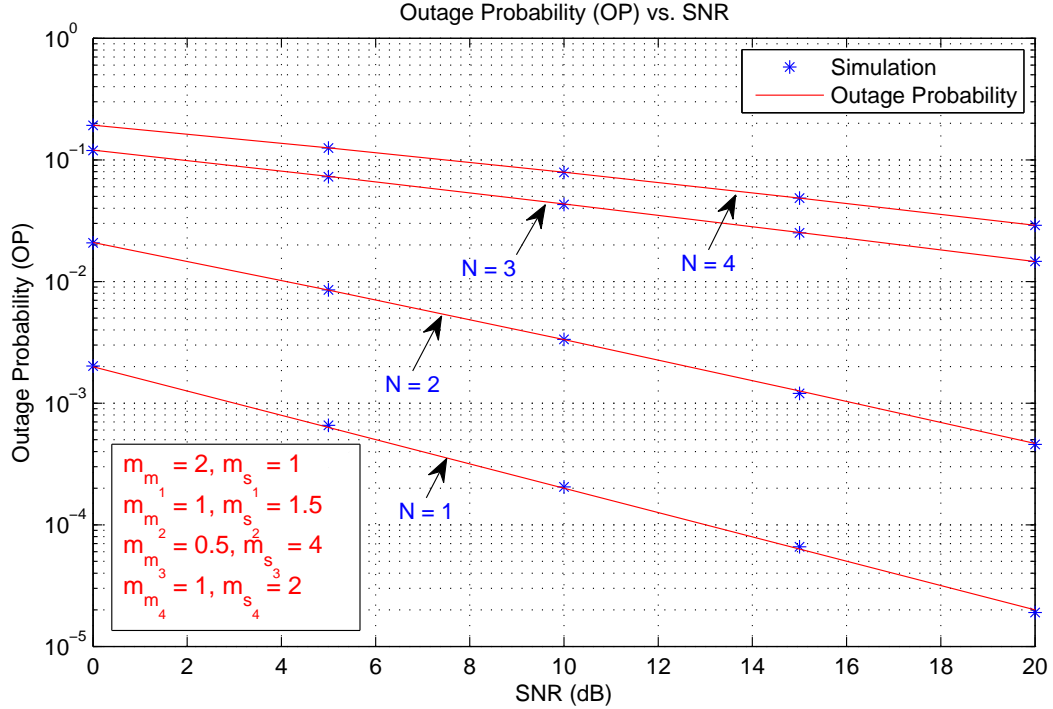
the OP increases.

Figure III.3: Outage Probability (OP) with respect to varying SNRs for different (N) number of hops with i.n.i.d. channels having $m_{m_1} = 2$, $m_{m_2} = 1$, $m_{m_3} = 0.5$, $m_{m_4} = 1$, $m_{s_1} = 1$, $m_{s_2} = 1.5$, $m_{s_3} = 4$, and $m_{s_4} = 2$.

Similar Monte Carlo simulations based on different thresholds and also for a 3-D plot having effects with both the varying SNRs as well as thresholds are demonstrated next. The basic results were presented above. Now, some additional and informative Monte Carlo simulation results are presented for more insight.

Outage probability (OP) based on varying threshold's can be seen in the following figure III.4. (III.5) has been verified and compared against the Monte Carlo simulation. The different specifications considered in the Monte Carlo simulations for OP were varying threshold from $\gamma_{th} = 0.001$ through $\gamma_{th} = 10$, and a SNR of 25 dB. As expected, we see that as the number of hops N increases and as the SNR decreases, the OP increases.
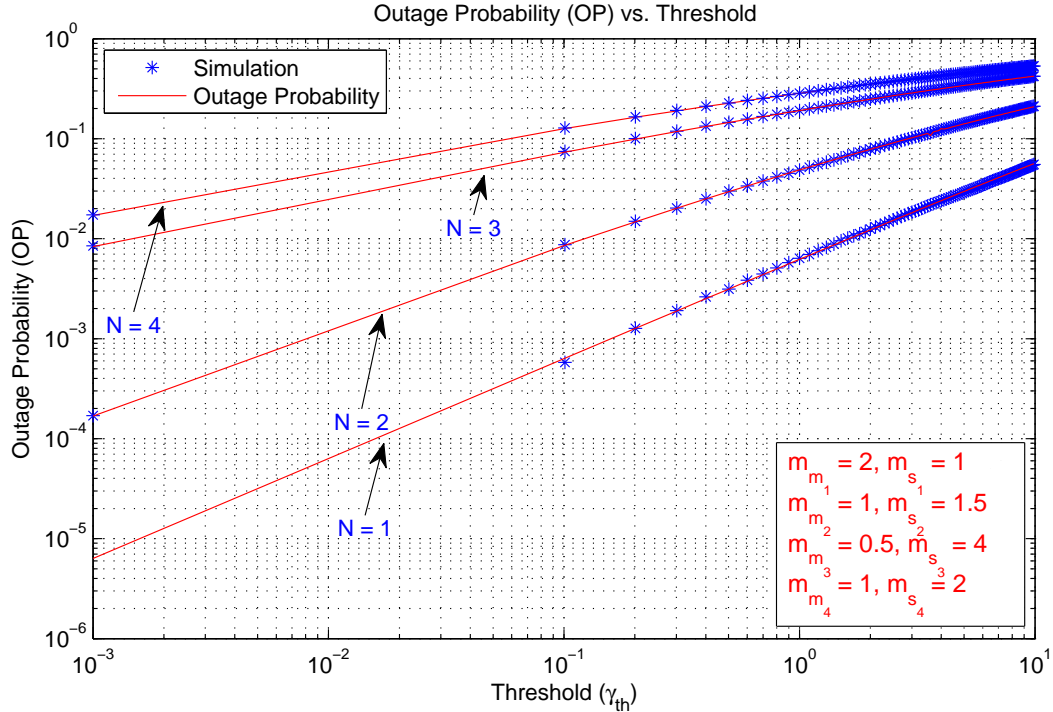
Figure III.4: OP with respect to varying thresholds for different (N) number of hops with i.n.i.d. channels having $m_{m_1} = 2$, $m_{m_2} = 1$, $m_{m_3} = 0.5$, $m_{m_4} = 1$, $m_{s_1} = 1$, $m_{s_2} = 1.5$, $m_{s_3} = 4$, and $m_{s_4} = 2$.

OP based on both varying SNRs as well as varying thresholds can be seen in the following figure III.5. The different specifications considered in the Monte Carlo simulations for OP were as: varying SNR from 0 dB through 30 dB and varying threshold from $\gamma_{th} = 0.001$ through $\gamma_{th} = 2$. It can be seen that as the SNR increases and as the threshold decreases, better performance is achieved i.e. low OP is achieved.
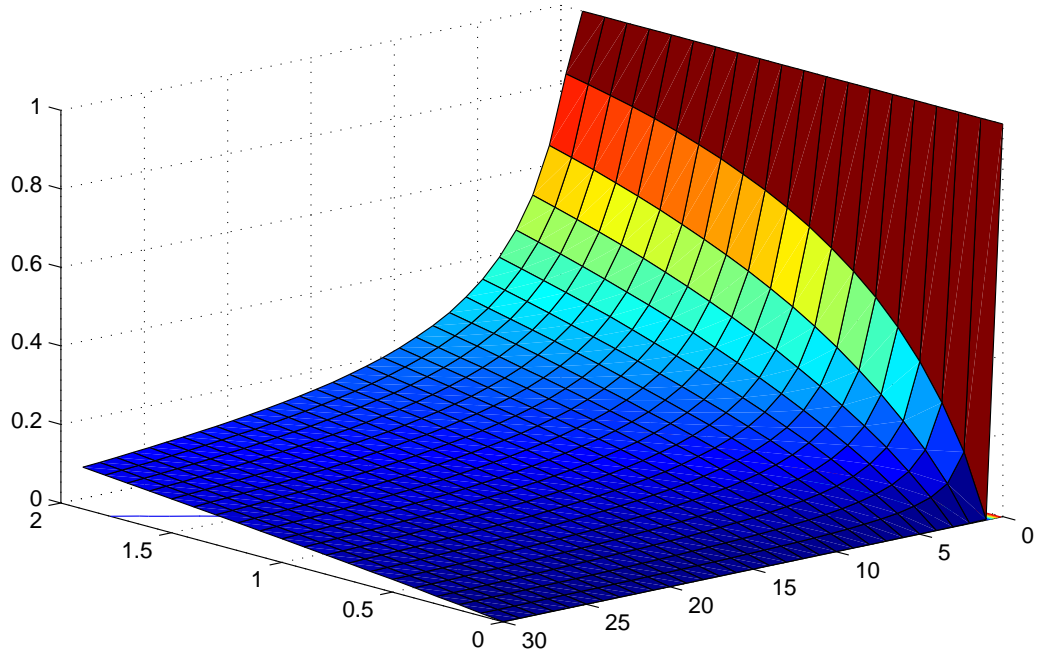
Figure III.5: OP with respect to varying both SNRs and thresholds with i.n.i.d. channels having $m_{m_1} = 2$, $m_{m_2} = 1$, $m_{m_3} = 0.5$, $m_{m_4} = 1$, $m_{s_1} = 1$, $m_{s_2} = 1.5$, $m_{s_3} = 4$, and $m_{s_4} = 2$.

Now with regards to BER, it can be observed for BPSK (as coherent case) and DPSK (as non-coherent case) modulation schemes from figures III.6 and III.7 respectively that as the number of hops N increases, the BER also increases, as expected. Additionally, as the SNR increases (varies from 0 dB through 20dB), the BER decreases expectedly. These results are in accordance with the numerical values acquired from MAPLE for the equations presented in (III.9) and (III.11), respectively.
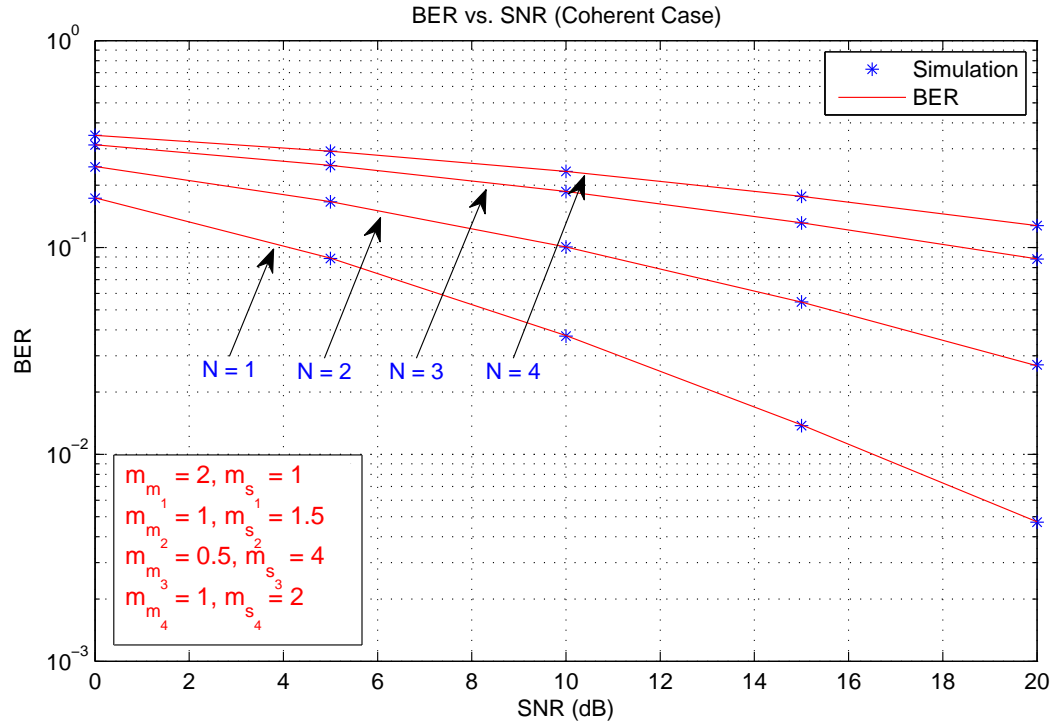
Figure III.6: BER for coherent modulation schemes (BPSK) for different (N) number of hops with i.n.i.d. channels having $m_{m_1} = 2$, $m_{m_2} = 1$, $m_{m_3} = 0.5$, $m_{m_4} = 1$, $m_{s_1} = 1$, $m_{s_2} = 1.5$, $m_{s_3} = 4$, and $m_{s_4} = 2$.
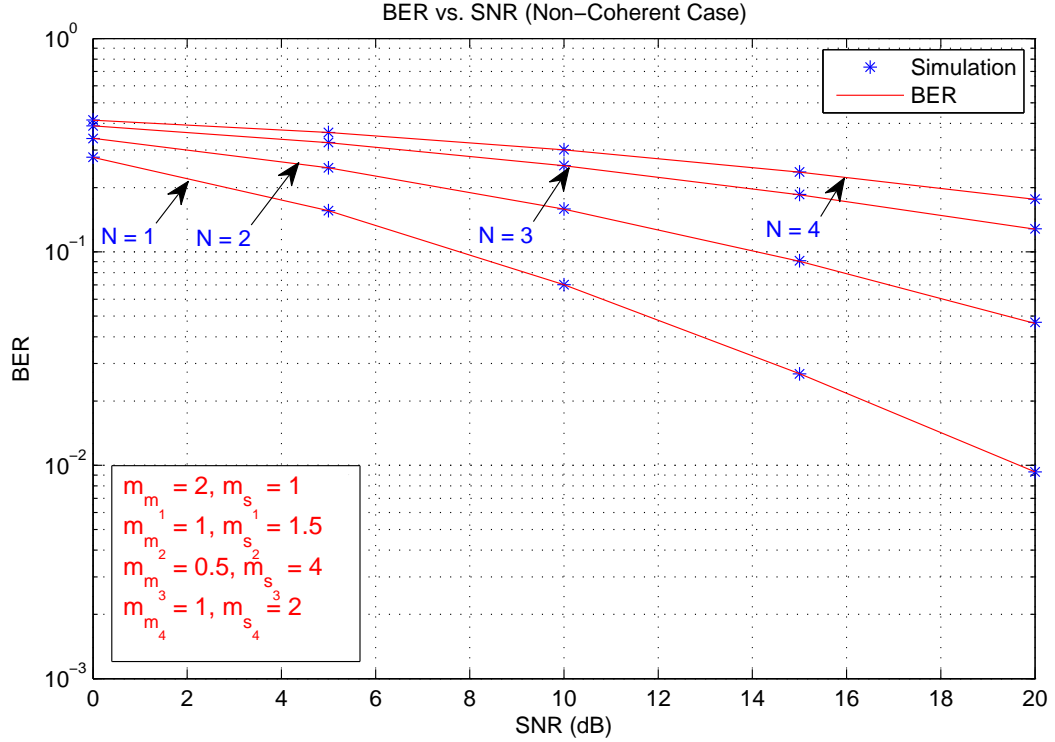
Figure III.7: BER for non-coherent modulation schemes (DPSK) for different (N) number of hops with i.n.i.d. channels having $m_{m_1} = 2$, $m_{m_2} = 1$, $m_{m_3} = 0.5$, $m_{m_4} = 1$, $m_{s_1} = 1$, $m_{s_2} = 1.5$, $m_{s_3} = 4$, and $m_{s_4} = 2$.

Furthermore, it can be observed from figure III.8 that as the number of hops N increases, the EC decreases due to loss of power from hop-to-hop. Additionally, as the SNR increases (varies from -5 dB through 40 dB), the EC increases. These results are in accordance with the numerical values acquired from MAPLE for the EC expression acquired in (III.13).
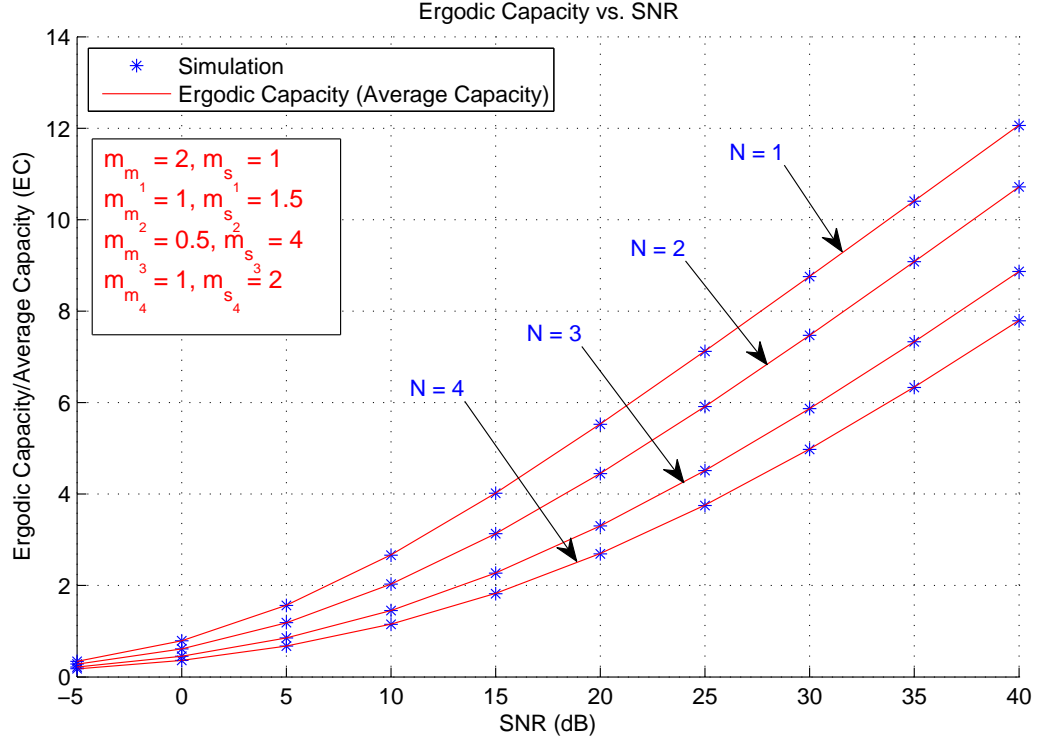
Figure III.8: Ergodic Capacity (Average Capacity) for different (N) number of hops with i.n.i.d. channels having $m_{m_1} = 2$, $m_{m_2} = 1$, $m_{m_3} = 0.5$, $m_{m_4} = 1$, $m_{s_1} = 1$, $m_{s_2} = 1.5$, $m_{s_3} = 4$, and $m_{s_4} = 2$.

III.5   Conclusion

Previous analysis of the performance of multihop relay networks in cascaded GK composite fading channels has relied on a MGF based approach. In this chapter, the exact expression for the distribution of the end-to-end SNR PDF in cascaded GK composite fading channels is derived utilizing the umbrella of Fox H-function extensively. Next, closed-form expressions for the subsequent performance metrics like OP, BER for both coherent and non-coherent modulation schemes, and EC were presented. The obtained results conform with the Monte Carlo simulation results.

Chapter IV

An Exact Closed-Form Expression for the BER of Binary Modulations with Dual-Branch Selection over Generalized-K Composite Fading Channels

Studying different diversity schemes has marked its importance among the researchers as it undoubtedly increases the efficiency of the communication system. Hence, this chapter discusses similar issue and proceeds as follows. A brief overview on the related work in terms of diversity schemes is presented followed by the specific model used for the communication system in this problem. Finally, the actual bit error rate (BER) analysis is presented in exact closed-form involving the interesting extended generalized bivariate Meijer G function (EGBMGF) (refer Appendix B).

IV.1 Related Work

Using the Nakagami multipath fading model that is versatile enough to model various multipath fading conditions ranging from severe fading to non-fading scenario, and the Gamma model for shadowing has led to the generalized-K (Gamma-Gamma) composite fading model [18], [21]-[24]. As mentioned in Chapter II, generalized-K (GK) distribution, earlier used in radar applications and recently being used in the context of wireless digital communications over fading channels, is one of the relatively new tractable models used to describe the statistical behavior of multipath fading and shadowing effects as compared to log-normal based models. GK fading model is quite general model as it includes K-distribution as its special case and accurately approximates many other fading models such as Nakagami-m and Rayleigh-Lognormal (R-L) ([22] and references therein). Finally, GK distribution is a distribution of the product of two independent Gamma random variables (RV) and hence is a special case of the Fox H-function and in turn a special case of Meijer G-function where the product of two Meijer G-function's can be represented in terms of a EGBMGF [26].

It is noteworthy to mention that BER is one of the most important performance measures that forms the basis in designing wireless communication systems. Based on the open technical literature and up to the best of our knowledge, error analysis has been performed for dual diversity with selection combining (SC) over log-normal fading channels in closed-form using moment generating function (MGF) based approach in [40] and with Weibull fading channel as an approximate using characteristic function (CF) based approach in [41]. Additionally, error performance analysis of SC systems with independent and identically distributed (i.i.d.) GK fading branches was performed in [42] involving integral form expressions. Further, in [43] the analysis was performed for dual-branch SC citing the difficulty in deriving the expression for the probability density function (PDF). This issue was tackled in [8] for an arbitrary number of branches and the authors therein have described and utilized a method to

perform the BER analysis directly from the cumulative density function (CDF) eliminating the need of deriving the PDF and relying on the Gauss-Laguerre quadrature technique.

In this work, this problem has been revisited under the umbrella of the H-functions and an exact closed-form expression of the BER of binary modulation systems with dual-branch SC scheme and undergoing GK fading where the channels are independent but not necessarily identically distributed (i.n.i.d.) was derived. The remainder of the chapter is organized as follows. Section two introduces the system model. Next, section three presents the analytical BER analysis, and finally, section four discusses the results and summarizes the chapter.

IV.2   Specific Model

The system model considered is described as follows. A SC based communication system with a source and a destination is considered with i.n.i.d. channels as follows

$$Y = \alpha X + n, \tag{IV.1}$$

where Y is the received signal at the receiver end, X is the transmitted signal, α is the channel gain, and n is the additive white Gaussian noise (AWGN). Following channel properties and statistical characteristics remain similar to as described earlier in Chapter II.

IV.3 BER Analysis

In SC combining scheme, the highest SNR branch is selected. In this case, for dual-diversity, the SNR, γ_{sc}, is given by

$$\gamma_{sc} = \max(\gamma_1, \gamma_2). \tag{IV.2}$$

The CDF of γ_{sc} is given by

$$F(\gamma_{sc}) = Pr(\max(\gamma_1, \gamma_2) \le \gamma_{sc}) = \prod_{n=1}^{2} F_{\gamma_n}(\gamma_{sc}). \tag{IV.3}$$

The BER for SC is given by

$$P_e = \int_0^\infty P_e\left(\epsilon|\gamma_{sc}\right) f_{\gamma_n}\left(\gamma\right) d\gamma_{sc} = \int_0^\infty P_e\left(\epsilon|\gamma_{sc}\right) dF_{\gamma_n}\left(\gamma_{sc}\right), \tag{IV.4}$$

where $P_e\left(\epsilon|\gamma_{sc}\right)$ is the conditional error probability (CEP) for the given SNR. A unified CEP expression for coherent and non-coherent binary modulation schemes over an AWGN channel is given in [44] as

$$P_e\left(\epsilon|\gamma_{sc}\right) = \frac{\Gamma(p, q\gamma_{sc})}{2\Gamma(p)}, \tag{IV.5}$$

where $\Gamma(\cdot, \cdot)$ is the complementary incomplete gamma function [27, Eq. (8.350.2)]. The parameters p and q in (IV.5) account for different modulation schemes. For an extensive list of modulation schemes represented by these parameters, one may look into [45] or as shown in table IV.1.

Now, applying integration by parts in (IV.4), we get

$$P_e = P_e\left(\epsilon|\gamma_{sc}\right) F(\gamma_{sc})|_0^\infty - \int_0^\infty F(\gamma_{sc}) dP_e\left(\epsilon|\gamma_{sc}\right). \tag{IV.6}$$

Table IV.1: Conditional Error Probability (CEP) Parameters

Modulation	p	q
Binary Frequency Shift Keying (BFSK)	0.5	0.5
Binary Phase Shift Keying (BPSK)	0.5	1
Differential Phase Shift Keying (DPSK)	1	1

The first term goes to zero using [46, Eq. (6.5.3)]. Further, substituting (IV.5) into (IV.6) and using [46, Eq. (6.5.25)], the average BER can be written as

$$P_e = \frac{q^p}{2\Gamma(p)} \int_0^\infty \exp(-q\gamma_{sc})\gamma_{sc}^{p-1} F(\gamma_{sc}) d\gamma_{sc}. \tag{IV.7}$$

On substituting (IV.3) in the above obtained expression, we get

$$P_e = \frac{q^p}{2\Gamma(p)} \int_0^\infty \exp(-q\gamma_{sc})\gamma_{sc}^{p-1} \prod_{n=1}^{2} F_{\gamma_n}(\gamma) d\gamma_{sc}. \tag{IV.8}$$

Using [26], we obtain the product of the CDFs present in the above expression in terms of EGBMGF as

$$\prod_{n=1}^{2} F_{\gamma_n}(\gamma) = F_{\gamma_1}(\gamma)F_{\gamma_2}(\gamma) = \kappa_1 \; S \left[\left\{ \begin{matrix} 0,0 \\ 0,0 \\ 2,1 \\ 1,0 \\ 2,1 \\ 1,0 \end{matrix} \right\} \middle| \begin{matrix} -;- \\ 1;\kappa_2 \\ 1;\kappa_3 \end{matrix} \middle| \begin{matrix} (\kappa_4)\,\gamma \\ (\kappa_5)\,\gamma \end{matrix} \right], \tag{IV.9}$$

where $S[\cdot]$ is the EGBMGF as given in [47, Eq. (2.1)], $\kappa_1 = \frac{1}{\Gamma(m_{m_1})\Gamma(m_{s_1})\Gamma(m_{m_2})\Gamma(m_{s_2})}$, $\kappa_2 = m_{m_1}, m_{s_1}, 0$, $\kappa_3 = m_{m_2}, m_{s_2}, 0$, $\kappa_4 = \frac{m_{m_1}m_{s_1}}{\Omega_{o_1}}$ and $\kappa_5 = \frac{m_{m_2}m_{s_2}}{\Omega_{o_2}}$. The above

expression can also be expressed as,

$$\prod_{n=1}^{2} F_{\gamma_n}(\gamma) = F_{\gamma_1}(\gamma) F_{\gamma_2}(\gamma) = \kappa_1 \; G_{0,0:1,3:1,3}^{0,0:2,1:2,1} \left(\left. \begin{array}{c|c|c} - & 1 & 1 \\ \hline - & \kappa_2 & \kappa_3 \end{array} \right| (\kappa_4 \gamma), (\kappa_5 \gamma) \right),$$

(IV.10)

where $G(\cdot)$ is EGBMGF as in [48]. Additionally, (IV.9) or (IV.10) can be represented as,

$$\prod_{n=1}^{2} F_{\gamma_n}(\gamma) = F_{\gamma_1}(\gamma) F_{\gamma_2}(\gamma) = \kappa_1$$

$$\times S \left[\left. \kappa_4 \gamma, \kappa_5 \gamma \; \right| \; \left[\begin{array}{c} 0,0 \\ 0,0 \end{array} \right] \; \left. \begin{array}{c} - \\ - \end{array} \right| \left(\begin{array}{c} 2,1 \\ 1,3 \end{array} \right) \; 1 \atop \kappa_2 \; \left| \; \left(\begin{array}{c} 2,1 \\ 1,3 \end{array} \right) \; 1 \atop \kappa_3 \right],$$

(IV.11)

where $S[\cdot]$ is EGBMGF as in [49, Eq. (4)].

Lemma 2 [47, Eq. (2.1)]: The integral involving the EGBMGF of two variables with an exponential term with the RV as one of its argument and a term with RV

itself evaluates to

$$
\int_0^\infty x^{\lambda-1} e^{-\mu x}\; S\left[\begin{array}{c} \begin{bmatrix} p,0 \\ A-p,B \end{bmatrix} \\ \begin{pmatrix} q,r \\ C-q,D-r \\ k,l \\ E-k,F-l \end{pmatrix} \end{array} \left| \begin{array}{c} (a);(b) \\ (c);(d) \\ (e);(f) \end{array} \right| \begin{array}{c} \alpha x^\rho \\ \beta x^\rho \end{array} \right] dx
$$

$$
= (2\pi)^{\frac{1}{2}(1-\rho)} \frac{\rho^{\lambda-1/2}}{\mu^\lambda}\; S\left[\begin{array}{c} \begin{bmatrix} p+\rho,0 \\ A-p,B \end{bmatrix} \\ \begin{pmatrix} q,r \\ C-q,D-r \\ k,l \\ E-k,F-l \end{pmatrix} \end{array} \left| \begin{array}{c} \Delta(\rho,\lambda),(a);(b) \\ (c);(d) \\ (e);(f) \end{array} \right| \begin{array}{c} \frac{\alpha\rho^\rho}{\mu^\rho} \\ \frac{\beta\rho^\rho}{\mu^\rho} \end{array} \right],
$$

(IV.12)

where $\Delta(\rho,\lambda) = \frac{\lambda}{\rho}, \frac{\lambda+1}{\rho}, \cdots, \frac{\lambda+\rho-1}{\rho}$ [47, Eq. (1.7)].

Now, substituting (IV.9) or (IV.10) or (IV.11) into (IV.8), then using the Lemma 2 given above and performing additional manipulations (refer Appendix C), the desired closed-form expression for the average BER is obtained as

$$
P_e = \frac{\kappa_1}{2\Gamma(p)}\; S\left[\begin{array}{c} \begin{bmatrix} 1,0 \\ 0,0 \end{bmatrix} \\ \begin{pmatrix} 2,1 \\ 1,0 \\ 2,1 \\ 1,0 \end{pmatrix} \end{array} \left| \begin{array}{c} p \\ 1;\kappa_2 \\ 1;\kappa_3 \end{array} \right| \begin{array}{c} \frac{(\kappa_4)}{q} \\ \frac{(\kappa_5)}{q} \end{array} \right],
$$

(IV.13)

or equivalently

$$P_e = \frac{\kappa_1}{2\Gamma(p)} \, G^{1,0:2,1:2,1}_{1,0:1,3:1,3} \left(p \left| \begin{array}{c} 1 \\ \\ \kappa_2 \end{array} \right| \begin{array}{c} 1 \\ \\ \kappa_3 \end{array} \left| (\kappa_4)\frac{1}{q}, (\kappa_5)\frac{1}{q} \right. \right),$$
(IV.14)

or equivalently

$$P_e = \frac{\kappa_1}{2\Gamma(p)} \, S \left[\frac{\kappa_4}{q}, \frac{\kappa_5}{q} \left| \begin{bmatrix} 1,0 \\ 1,0 \end{bmatrix} \right| p \left| \begin{pmatrix} 2,1 \\ 1,3 \end{pmatrix} \frac{1}{\kappa_2} \right| \begin{pmatrix} 2,1 \\ 1,3 \end{pmatrix} \frac{1}{\kappa_3} \right].$$
(IV.15)

IV.4 Results and Discussion

The numerical results for BER of SC scheme with dual-diversity over i.n.i.d. GK fading channels are presented in this section.

The exact solution presented above in (IV.13), (IV.14) and/or (IV.15) has not been found computable and hence its computability/evaluation was implemented using Mathematica as can be seen in Appendix B. This computability, therefore, has been utilized for different digital modulation schemes and is employed to discuss the results in comparison to respective Monte Carlo simulation outcomes.

The average SNR per bit in all the scenarios discussed is assumed to be equal. In addition, different digital modulation schemes are represented based on the values of p and q where $p = 0.5$ and $q = 1$ represents binary phase shift keying (BPSK), $p = 1$ and $q = 1$ represents differential phase shift keying (DPSK) and binary frequency shift keying (BFSK) is represented by $p = 0.5$ and $q = 0.5$. In Monte Carlo simulations, the GK fading channel was generated by the product of two independent gamma RVs.

We observe from figures IV.1, IV.2, and IV.3 that this implemented computability of EGBMGF provides a perfect match to the MATLAB simulated results and the results are as expected i.e. the BER increases as the shadowing effect increases (i.e. value of m_s decreases) while keeping multipath fading constant at $m_m = 1$. The

figures shown respectively represent BPSK, BFSK, and DPSK. Its important to note here that these values for the parameters were selected randomly to prove the validity of the obtained results and hence specific values based on the standards can be used to obtain the required results.
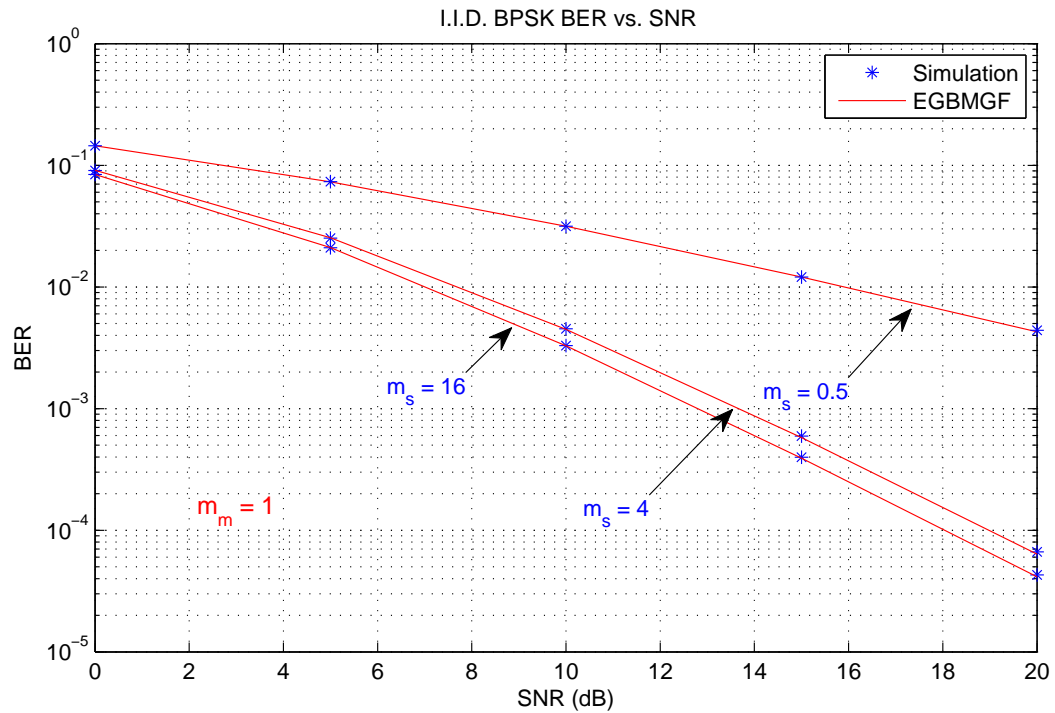
Figure IV.1: I.I.D. BPSK BER for $m_m = 1$ and varying m_s.
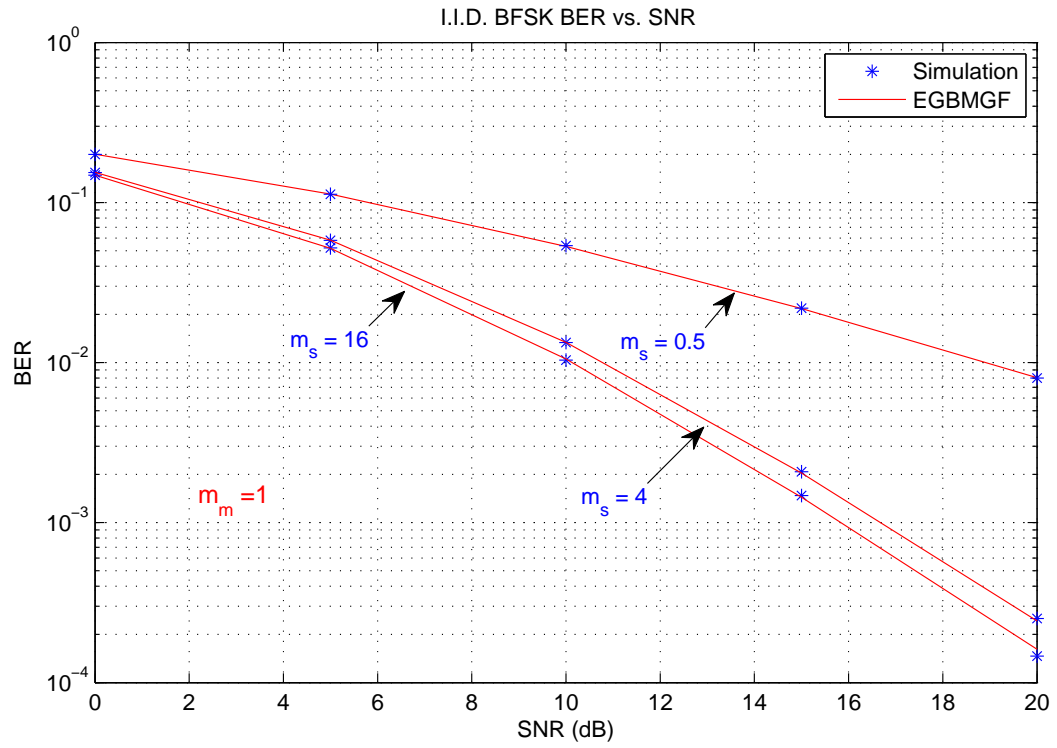
Figure IV.2: I.I.D. BFSK BER for $m_m = 1$ and varying m_s.
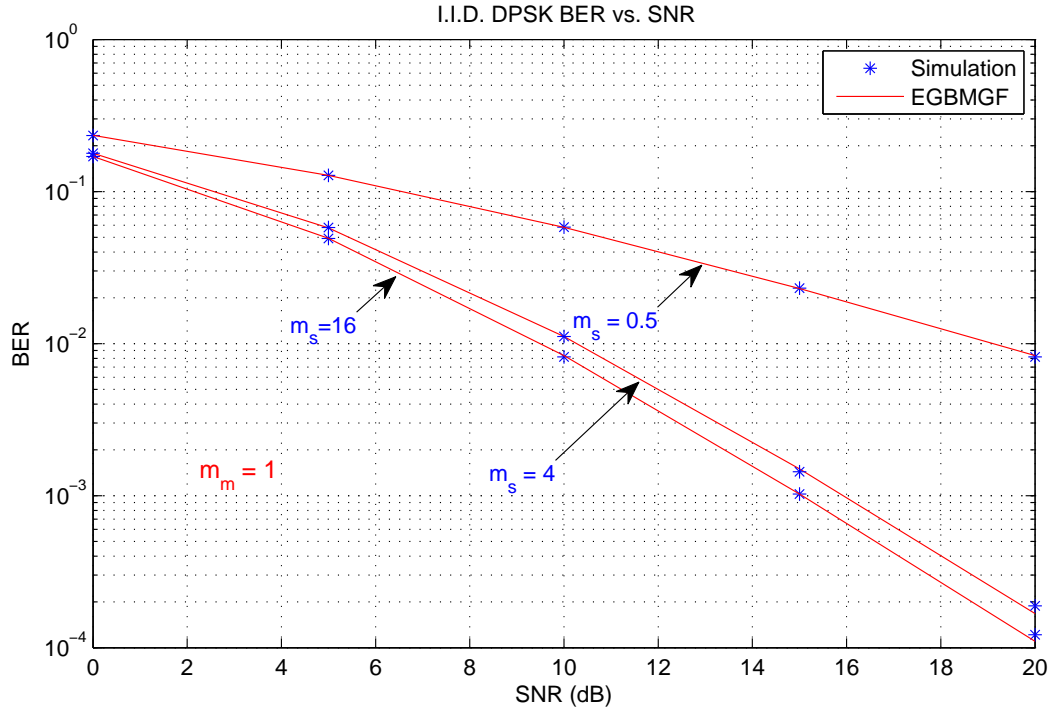
Figure IV.3: I.I.D. DPSK BER for $m_m = 1$ and varying m_s.

Similarly, keeping shadowing effect constant at $m_s = 2$ and varying the multipath fading, following expected results are observed for BPSK as demonstrated in figure IV.4. It shows that the BER increases as the effect of multipath fading increases (i.e. value of m_m decreases) while keeping the shadowing effect constant.
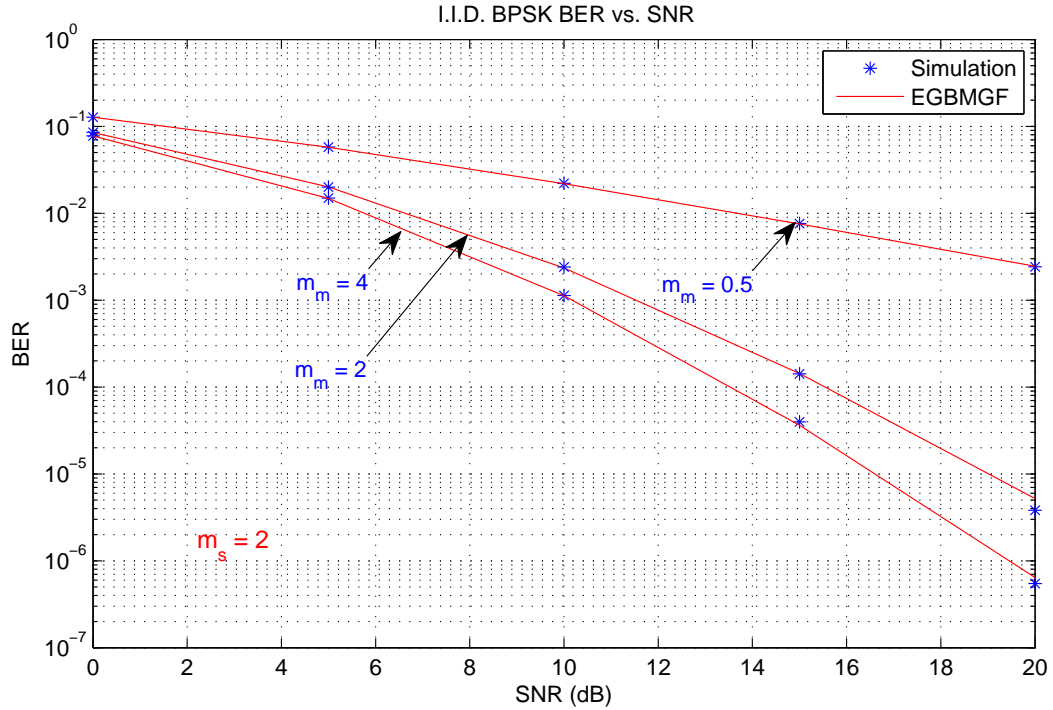
Figure IV.4: I.I.D. BPSK BER for varying m_m and $m_s = 2$.

Furthermore, to demonstrate the case that the results presented in this chapter also handle the presence of i.n.i.d. GK channels, following figure IV.5 presents the different modulation schemes with different effects of multipath fading and shadowing on both their channels. The values utilized for multipath fading and shadowing were as follows; $m_{m_1} = 1$, $m_{m_2} = 2$, $m_{s_1} = 0.5$, and $m_{s_2} = 4$. It can be seen that, as expected, BPSK outperforms the other modulation schemes and BFSK and DPSK perform in similar fashion at lower SNR whereas as the SNR increases DPSK performs better than BFSK.
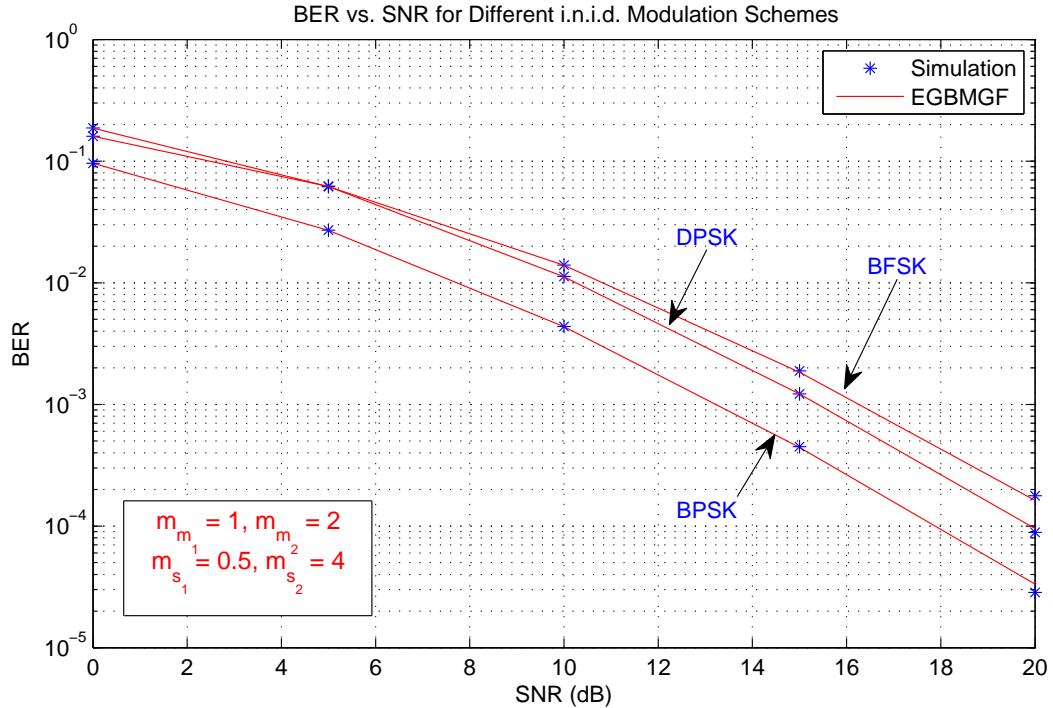
Figure IV.5: BER for different modulation schemes undergoing i.n.i.d. channels with $m_{m_1} = 1$, $m_{m_2} = 2$, $m_{s_1} = 0.5$, and $m_{s_2} = 4$.

Similar results for any other values of $m'_m s$ and $m'_s s$ can be observed for the exact closed-form BER for dual-diversity i.n.i.d. GK channels presented in this chapter.

IV.5   Conclusion

An exact closed-form expression for the BER performance of different binary modulations with dual-branch SC scheme over i.n.i.d. GK fading was derived. The analytical calculations were done utilizing a general class of special functions, specifically, the EGBMGF. In addition, this chapter presents numerical examples to illustrate the mathematical formulation developed in this work and to show the effect of the fading and shadowing severity and unbalance on the system performance.

Chapter V

Concluding Remarks

V.1   Summary

This work was motivated by the new modeling problems that the emerging communication systems have spurred and the subsequent role of such models in the performance of these communication systems. In this thesis, some of the tools needed to model and further analyze the performance of different communication systems have been developed. First, the characterization of composite fading channels is considered where the generalized-K (GK) composite fading model is introduced and some of its statistical characteristics were proposed.

In Chapter III,we applied the GK model to cascaded channels to analyze its end-to-end signal-to-noise ratio (SNR). Next, the performance metrics for these independent but not necessarily identical (i.n.i.d.) cascaded channels undergoing GK fading were analyzed. These metrics included outage probability (OP), bit error rate (BER), and ergodic capacity (EC). This chapter demonstrated that such type of similar analysis can be done via simpler methods and approaches with the help of special functions and their extensive and extremely useful properties.

Then in Chapter IV, the same model was employed to analyze the BER of a

dual-diversity system with selection combining scheme undergoing i.n.i.d. GK fading channels. The results were presented in terms of extended generalized bivariate Meijer G-function (EGBMGF). Although these types of special functions do not seem to be that useful, if computable, this view changes to a positive one. Hence, the computability of this EGBMGF was tackled using Mathematica and is present in the appendices of this thesis. The outcome of this chapter along with the computability of EGBMGF opens up new horizons as well as broadens up the current scope of research work in this field of study.

V.2   Future Research Work

The work presented in this thesis can be extended in the following directions.

With the computability of extended generalized bivariate Meijer G-function (EGBMGF), the presented results can be extended to the dual-diversity of chain of nodes or in other words dual-diversity of cascaded channels.

Moreover, the extension can be in the direction of analyzing different performance metrics for the model utilized in Chapter IV and also for the model that is mentioned above i.e. involving dual-diversity of cascaded channels.

Another possible extension is studying the different diversity techniques such as switching diversity and maximal ratio combining, among others, to both the models discussed above.

We also observe that having the computability of EGBMGF in a very generalized form, this might allow to look into multivariate form of Meijer G-function. If this comes out to be tractable then undoubtedly we will see much more possible research study openings further in this track. In addition, this will allow to analyze the communication systems in a rather simpler form relative to other techniques being employed traditionally.

APPENDICES

Appendix A

The H-Function Distribution Family

Definition: The H-function can be defined as

$$
\begin{aligned}
&\mathrm{H}_{p,q}^{m,n}\left[z \;\middle|\; \begin{array}{l} (a_1,\alpha_1),\ldots,(a_p,\alpha_p) \\ (b_1,\beta_1),\ldots,(b_q,\beta_q) \end{array}\right] = \\
&\frac{1}{2\pi i}\int_C \frac{\prod_{j=1}^m \Gamma(b_j-\beta_j s)\prod_{j=1}^n \Gamma(1-a_j+\alpha_j s)}{\prod_{j=m+1}^q \Gamma(1-b_j+\beta_j s)\prod_{j=n+1}^q \Gamma(a_j-\alpha_j s)} z^s ds,
\end{aligned}
\tag{A.1}
$$

where $0 \le m \le q$, $0 \le n \le p$, $\alpha_j > 0$, and $\beta_j > 0$ and $a_j(j=1,2,\ldots,p)$ and $b_j(j=1,2,\ldots,q)$ are complex numbers such that no pole of $\Gamma(b_j-\beta_j s)$ for $j=1,2,\ldots,m$ coincides with with any pole of $\Gamma(1-a_j+\alpha_j s)$ for $j=1,2,\ldots,n$. The contour C is a straight line parallel to the imaginary axis in the complex plane and the poles of $\Gamma(b_j-\beta_j s)$ lie on the right of C while those of $\Gamma(1-a_j+\alpha_j s)$ lie on the left of C.

Many of the so-called special functions are special cases of the H-function, including Gauss and confluent hypergeometric functions, MacRobert E-function, Meijer function, and Bessel functions [28, 50].

The Meijer G-function can be expressed as

$$
G_{p,q}^{m,n}\left[z \left|\begin{array}{c} a_1,\ldots,a_p \\ b_1,\ldots,b_q \end{array}\right.\right] = H_{p,q}^{m,n}\left[z \left|\begin{array}{c} (a_1,1),\ldots,(a_p,1) \\ (b_1,1),\ldots,(b_q,1) \end{array}\right.\right].
\tag{A.2}
$$

Definition: The *H*-function distribution can be expressed as

$$
p(x) = k\ H_{p,q}^{m,n}\left[cx \left|\begin{array}{c} (a_1,\alpha_1),\ldots,(a_p,\alpha_p) \\ (b_1,\beta_1),\ldots,(b_q,\beta_q) \end{array}\right.\right], x > 0,
\tag{A.3}
$$

where k and c are the parameters of the distribution such that $\int_0^\infty p(x)dx = 1$.

The characteristic function of the *H*-function distribution can be derived as [2]

$$
\phi(t) = \frac{k}{c}\ H_{q,p+1}^{n+1,m}\left[-\frac{i}{c}x \left|\begin{array}{c} (0,1)(1-a_1-\alpha_1,\alpha_1),\ldots,(1-a_p-\alpha_p,\alpha_p) \\ (1-b_1-\beta_1,\beta_1),\ldots,(1-b_q-\beta_q,\beta_q) \end{array}\right.\right], x > 0.
\tag{A.4}
$$

Many non-negative distributions are special cases of the *H*-function including the Gamma distribution, the Weibull distribution, the Beta distribution, the Rayleigh distribution, and the general hypergeometric distribution. As an instance, the general hypergeometric distribution expressed in terms of Meijer *G*-function and hence in terms of *H*-function is shown below in (A.5).

$$
\begin{aligned}
{}_pF_q\left(\begin{array}{c} a_p \\ b_q \end{array}\middle| z\right) &= \frac{\Gamma(a_p)}{\Gamma(b_q)}\ G_{p,q+1}^{p,1}\left(\begin{array}{c} 1-a_p \\ 0,1-b_q \end{array}\middle| -z\right) \\
&= \frac{\Gamma(a_p)}{\Gamma(b_q)}\ H_{p,q+1}^{p,1}\left(\begin{array}{c} (1-a_p,1) \\ (0,1),(1-b_q,1) \end{array}\middle| -z\right).
\end{aligned}
\tag{A.5}
$$

Similarly, other distributions can be expressed in such similar form.

Appendix B

Extended Generalized Bivariate Meijer G-Function

B.1   Definition

The extended generalized bivariate Meijer G-function (EGBMGF) can be defined in any of the following ways.

Representation 1: Based on [47]

$$
S\begin{bmatrix} x \\ y \end{bmatrix} \equiv S \left[\begin{bmatrix} \begin{bmatrix} p,0 \\ A-p,B \end{bmatrix} \\ \begin{Bmatrix} q,r \\ C-q,D-r \end{Bmatrix} \\ \begin{Bmatrix} k,l \\ E-k,F-l \end{Bmatrix} \end{bmatrix} \middle| \begin{matrix} (a);(b) \\ (c);(d) \\ (e);(f) \end{matrix} \middle| \begin{matrix} x \\ y \end{matrix} \right] \tag{B.1}
$$

$$
= \frac{1}{(2\pi i)^2} \int_{C_1} \int_{C_2} \frac{\prod_{j=1}^{p}\Gamma(a_j+s+t)\prod_{j=1}^{q}\Gamma(1-c_j+s)}{\prod_{j=p+1}^{A}\Gamma(1-a_j-s-t)\prod_{j=1}^{B}\Gamma(b_j+s+t)}
$$

$$
\cdot \frac{\prod_{j=1}^{r}\Gamma(d_j-s)\prod_{j=1}^{k}\Gamma(1-e_j+t)\prod_{j=1}^{l}\Gamma(f_j-t)}{\prod_{j=q+1}^{C}\Gamma(c_j-s)\prod_{j=r+1}^{D}\Gamma(1-d_j+s)\prod_{j=k+1}^{E}\Gamma(e_j-t)}
$$

$$
\cdot \frac{x^s y^t \, ds \, dt}{\prod_{j=l+1}^{F}\Gamma(1-f_j+t)},
$$

where $A+C<B+D$, $A+E<B+F$.

Representation 2: Based on [49]

$$
S\begin{bmatrix} x \\ y \end{bmatrix} \equiv S\left[x,y \middle| \begin{bmatrix} m_1,0 \\ p_1,q_1 \end{bmatrix} \begin{matrix} a_{p_1} \\ b_{q_1} \end{matrix} \middle| \begin{pmatrix} n_2,m_2 \\ p_2,q_2 \end{pmatrix} \begin{matrix} c_{p_2} \\ d_{q_2} \end{matrix} \middle| \begin{pmatrix} n_3,m_3 \\ p_3,q_3 \end{pmatrix} \begin{matrix} e_{p_3} \\ f_{q_3} \end{matrix} \right]
$$

$$
\equiv G^{m_1,0:n_2,m_2:n_3,m_3}_{p_1,q_1:p_2,q_2:p_3,q_3}\left(\begin{matrix} a_1,\ldots,a_{p_1} \\ b_1,\ldots,b_{q_1} \end{matrix} \middle| \begin{matrix} c_1,\ldots,c_{p_2} \\ d_1,\ldots,d_{q_2} \end{matrix} \middle| \begin{matrix} e_1,\ldots,e_{p_3} \\ f_1,\ldots,f_{q_3} \end{matrix} \middle| x,y \right) \tag{B.2}
$$

$$
= \frac{1}{(2\pi i)^2} \int_{C_1} \int_{C_2} \frac{\prod_{j=1}^{m_1}\Gamma(a_j+s+t)\prod_{j=1}^{m_2}\Gamma(1-c_j+s)}{\prod_{j=m_1+1}^{p_1}\Gamma(1-a_j-s-t)\prod_{j=1}^{q_1}\Gamma(b_j+s+t)}
$$

$$
\cdot \frac{\prod_{j=1}^{n_2}\Gamma(d_j-s)\prod_{j=1}^{m_3}\Gamma(1-e_j+t)\prod_{j=1}^{n_3}\Gamma(f_j-t)}{\prod_{j=m_2+1}^{p_2}\Gamma(c_j-s)\prod_{j=n_2+1}^{q_2}\Gamma(1-d_j+s)\prod_{j=m_3+1}^{p_3}\Gamma(e_j-t)}
$$

$$
\cdot \frac{x^s y^t \, ds \, dt}{\prod_{j=n_3+1}^{q_3}\Gamma(1-f_j+t)},
$$

where C_1 and C_2 are two suitable contours and positive integers p_1, p_2, p_3, q_1, q_2, q_3,

m_1, m_2, m_3, n_2, and n_3 satisfy the following inequalities. $q_2 \geq 1$, $q_3 \geq 1$, $p_1 \geq 0$, $0 \leq m_1 \leq p_1$, $0 \leq m_2 \leq p_2$, $0 \leq n_2 \leq q_2$, $0 \leq m_3 \leq p_3$, $0 \leq n_3 \leq q_3$, $p_1 + p_2 \leq q_1 + q_2$, $p_1 + p_3 \leq q_1 + q_3$. The values $x = 0$ and $y = 0$ are excluded.

It is important to learn the relationship between both the representations shown above. Following equalities must be noted from both the above representations; $p = m_1$, $A = p_1$, $B = q_1$, $q = m_2$, $r = n_2$, $C = p_2$, $D = q_2$, $k = m_3$, $l = n_3$, $E = p_3$, and $F = q_3$.

B.2   Implementation

The EGBMGF was implemented in Mathemtica and the code is as shown below. With this implementation, the EGBMGF can be evaluated fast and accurately. An illustration along with the implementation code is demonstrated for its proper usage.

(*Extended Generalized Bivariate Meijer G-Function (EGBMGF)*)

Clear All;

(*Exception*)

S::Inconsistent Coeffs = "Inconsistent coefficients!";

$S[\{ast_-, bst_-\}, \{as_-, bs_-\}, \{at_-, bt_-\}, \{zs_-, zt_-\}] :=$ Module[{},

(*Gamma product terms with only $'s'$ as argument with other parameters*)

Pas = Function[u, Product[Gamma[1 − as[[1, n]] + u], {n, 1, Length[as[[1]]]}]];

Qas = Function[u, Product[Gamma[as[[2, n]] − u], {n, 1, Length[as[[2]]]}]];

Pbs = Function[u, Product[Gamma[bs[[1, n]] − u], {n, 1, Length[bs[[1]]]}]];

Qbs = Function[u, Product[Gamma[1 − bs[[2, n]] + u], {n, 1, Length[bs[[2]]]}]];

Ms = Function[u, Pas[u]Pbs[u]/(Qas[u]Qbs[u])];

(*Gamma product terms with only $'t'$ as argument with other parameters*)

Pat = Function[u, Product[Gamma[$1 - \text{at}[[1, n]] + u$], $\{n, 1, \text{Length}[\text{at}[[1]]]\}$]];

Qat = Function[u, Product[Gamma[$\text{at}[[2, n]] - u$], $\{n, 1, \text{Length}[\text{at}[[2]]]\}$]];

Pbt = Function[u, Product[Gamma[$\text{bt}[[1, n]] - u$], $\{n, 1, \text{Length}[\text{bt}[[1]]]\}$]];

Qbt = Function[u, Product[Gamma[$1 - \text{bt}[[2, n]] + u$], $\{n, 1, \text{Length}[\text{bt}[[2]]]\}$]];

Mt = Function[u, Pat[u]Pbt[u]/(Qat[u]Qbt[u])];

(*Gamma product terms with only $'s + t'$ as argument with other parameters*)

Past = Function[u, Product[Gamma[$\text{ast}[[1, n]] + u$], $\{n, 1, \text{Length}[\text{ast}[[1]]]\}$]];

Qast = Function[u, Product[Gamma[$1 - \text{ast}[[2, n]] - u$], $\{n, 1, \text{Length}[\text{ast}[[2]]]\}$]];

Qbst = Function[u, Product[Gamma[$\text{bst}[[2, n]] + u$], $\{n, 1, \text{Length}[\text{bst}[[2]]]\}$]];

Mst = Function[u, Past[u]/(Qast[u]Qbst[u])];

(*Contour limiters(Depends on numerator Gamma arguments

i.e. it must be half of the least valued Gamma arguments)*)

Rs = 1/4;

Rt = 1/4;

(*Assignments and Declarations*)

Zs = zs;

Zt = zt;

$W = 50$;

(*Final Evaluation*)

Print["Numerical Integration:"];

value = $\frac{1}{(2\pi I)^2}$NIntegrate[MT[s, t]Zs^{s}Zt^t, $\{s, \text{Rs} - IW, \text{Rs} + IW\}$,

$\{t, \text{Rt} - IW, \text{Rt} + IW\}$];

(*Returning back the value*)

Return[value];

];

(*End of EGBMGF*)

Here is an example of employing this implemented EGBMGF.

(*Testing*)

(*Declarations*)

$p = 0.5; q = 1;$

$mm1 = 1; ms1 = 2; mm2 = 1; ms2 = 2;$

$\Omega1 = 1; \Omega2 = 1;$

$snr = 10^{\wedge}(15/10)(*SNR = 0 - 20dBs*);$

(*Invoking the implemented EGBMGF module*)

$B = \frac{1}{2\text{Gamma}[p]\text{Gamma}[mm1]\text{Gamma}[ms1]\text{Gamma}[mm2]\text{Gamma}[ms2]} S[\{\{\{p\}, \{\}\}, \{\{\}, \{\}\}\},$

$\{\{\{1\}, \{\}\}, \{\{mm1, ms1\}, \{0\}\}\},$

$\{\{\{1\}, \{\}\}, \{\{mm2, ms2\}, \{0\}\}\},$

$\left\{ \frac{mm1\ ms1}{\Omega1\ snr\ q}, \frac{mm2\ ms2}{\Omega2\ snr\ q} \right\}]$

(*END*)

$\text{Out} = 0.00102393 - 7.09829 \times 10^{-16}i$

It is important to learn the relationship between the representations shown in the previous section and the implemented code presented above. Following equalities must be noted from both the above representations and the implemented code; $(a) = a_{p_1} = ast_-$, $(b) = b_{q_1} = bst_-$, $(c) = c_{p_2} = as_-$, $(d) = d_{q_2} = bs_-$, $(e) = e_{p_3} = at_-$, and $(f) = f_{q_3} = bt_-$.

Appendix C

Derivations of Some Equations

C.1 Derivation of the Outage Probability (OP) in (III.5)

Having (III.2), it is substituted in (III.4) and the following is obtained

$$P_{out} = \int_0^{\gamma_{th}} \prod_{n=1}^{N} \left(\frac{m_{m_n} m_{s_n}}{\Gamma(m_{m_n}) \Gamma(m_{s_n}) \Omega_{0_n}} \right) G_{0,2N}^{2N,0} \left[\prod_{n=1}^{N} \left(\frac{m_{m_n} m_{s_n}}{\Omega_{0_n}} \right) y \middle| \kappa_1 \right] dy, y > 0,$$

(C.1)

where $\kappa_1 = (m_{m_1} - 1), (m_{s_1} - 1), \ldots, (m_{m_N} - 1), (m_{s_N} - 1)$.

Now, using [29, Eq. (26)], the integral simplifies to

$$P_{out} = \prod_{n=1}^{N} \left(\frac{m_{m_n} m_{s_n}}{\Gamma(m_{m_n}) \Gamma(m_{s_n}) \Omega_{0_n}} \right) \gamma_{th} \, G_{1,2N+1}^{2N,1} \left[\prod_{n=1}^{N} \left(\frac{m_{m_n} m_{s_n}}{\Omega_{0_n}} \right) \gamma_{th} \middle| \begin{matrix} 0 \\ \kappa_1, -1 \end{matrix} \right].$$

(C.2)

This result can be further represented as

$$P_{out} = \prod_{n=1}^{N} \left(\frac{1}{\Gamma\left(m_{m_n}\right)\Gamma\left(m_{s_n}\right)} \right) \prod_{n=1}^{N} \left(\frac{m_{m_n} m_{s_n}}{\Omega_{0_n}} \right) \gamma_{th}$$
$$\times G_{1,2N+1}^{2N,1} \left[\prod_{n=1}^{N} \left(\frac{m_{m_n} m_{s_n}}{\Omega_{0_n}} \right) \gamma_{th} \left| \begin{matrix} 0 \\ \kappa_1, -1 \end{matrix} \right. \right]. \quad \text{(C.3)}$$

Now, utilizing [28, Eq. (6.2.4)], following final result is obtained

$$P_{out} = \prod_{n=1}^{N} \left(\frac{1}{\Gamma\left(m_{m_n}\right)\Gamma\left(m_{s_n}\right)} \right) G_{1,2N+1}^{2N,1} \left[\prod_{n=1}^{N} \left(\frac{m_{m_n} m_{s_n}}{\Omega_{0_n}} \right) \gamma_{th} \left| \begin{matrix} 1 \\ \kappa_3, 0 \end{matrix} \right. \right], \quad \text{(C.4)}$$

where $\kappa_3 = m_{m_1}, m_{s_1}, \ldots, m_{m_N}, m_{s_N}$.

C.2 Derivation for the Bit Error Rate (BER) in (IV.13)

As explained in Chapter 4, substituting (IV.9) or (IV.10) or (IV.11) into (IV.8) gives the following

$$P_e = \frac{q^p}{2\Gamma(p)} \int_0^\infty \exp(-q\gamma_{sc})\gamma_{sc}^{p-1} \kappa_1 \; S \left[\left\{ \begin{matrix} \begin{bmatrix} 0,0 \\ 0,0 \\ 2,1 \\ 1,0 \end{bmatrix} \\ 2,1 \\ 1,0 \end{matrix} \right| \begin{matrix} -;- \\ 1;\kappa_2 \\ 1;\kappa_3 \end{matrix} \left| \begin{matrix} (\kappa_4)\,\gamma \\ (\kappa_5)\,\gamma \end{matrix} \right. \right] d\gamma, \quad \text{(C.5)}$$

where $S[\cdot]$ is the extended generalized bivariate Meijer G-function (EGBMGF) as given in [47, Eq. (2.1)], $\kappa_1 = \frac{1}{\Gamma(m_{m_1})\Gamma(m_{s_1})\Gamma(m_{m_2})\Gamma(m_{s_2})}$, $\kappa_2 = m_{m_1}, m_{s_1}, 0$, $\kappa_3 = m_{m_2}, m_{s_2}, 0$, $\kappa_4 = \frac{m_{m_1} m_{s_1}}{\Omega_{o_1}}$ and $\kappa_5 = \frac{m_{m_2} m_{s_2}}{\Omega_{o_2}}$.

Now using the Lemma 2 on the above equation results into

$$P_e = \frac{q^p}{2\Gamma(p)} (2\pi)^{\frac{1}{2}(1-1)} \frac{1^{(p-\frac{1}{2})}}{q^p} \kappa_1 \ S \left[\begin{array}{c} \left[\begin{array}{c} 1,0 \\ 0,0 \end{array} \right] \\ \left\{ \begin{array}{c} 2,1 \\ 1,0 \\ 2,1 \\ 1,0 \end{array} \right. \end{array} \middle| \begin{array}{c} \Delta(1,p), -; - \\ 1; \kappa_2 \\ 1; \kappa_3 \end{array} \middle| \begin{array}{c} \frac{(\kappa_4)}{q} \\ \frac{(\kappa_5)}{q} \end{array} \right], \quad (C.6)$$

where $\Delta(1,p) = \frac{p}{1} = p$.

With further simplification, the final result is obtained as follows

$$P_e = \frac{1}{2\Gamma(p)} \kappa_1 \ S \left[\begin{array}{c} \left[\begin{array}{c} 1,0 \\ 0,0 \end{array} \right] \\ \left\{ \begin{array}{c} 2,1 \\ 1,0 \\ 2,1 \\ 1,0 \end{array} \right. \end{array} \middle| \begin{array}{c} p, -; - \\ 1; \kappa_2 \\ 1; \kappa_3 \end{array} \middle| \begin{array}{c} \frac{(\kappa_4)}{q} \\ \frac{(\kappa_5)}{q} \end{array} \right]. \quad (C.7)$$

Appendix D

Papers Submitted and Under Preparation

• I. S. Ansari, S. Al-Ahmadi, F. Yilmaz, M.-S. Alouini, and H. Yanikomeroglu, "An exact closed-form expression for the BER of binary modulations with dual-branch selection over Generalized-K fading", *Submitted to IEEE 73rd Vehicular Technology Conference: VTC 2011-Spring*, Budapest, Hungary.

• I. S. Ansari, S. Al-Ahmadi, F. Yilmaz, M.-S. Alouini, and H. Yanikomeroglu, "An exact closed-form expression for the BER and capacity of binary modulations with dual-branch selection over Generalized-K fading", *Submitted to IEEE Transactions on Communications*, Dec. 2010.

BIBLIOGRAPHY

[1] F. Yilmaz and M.-S. Alouini, "Product of the powers of generalized nakagami-m variates and performance of cascaded fading channels," in *IEEE Global Telecommunications Conference (GLOBECOM 2009)*, Honolulu, Hawaii, US, Nov. 2009, pp. 1–8.

[2] S. Al-Ahmadi, "Composite fading channel modeling and information capacity of distributed antenna architectures of cellular networks," Ph.D. dissertation, Carleton University, 2010.

[3] M. S. P. Kumar, P. Herhold, R. Bhattacharjee, and G. Fettweis, "Cooperative multi-hop relaying over fading channels using cascaded 2-hop technique," in *IEEE First India Annual Conference, 2004. Proceedings of the IEEE INDICON 2004*, India, Dec. 2004, pp. 139–142.

[4] J. B. Anderson, "Statistical distributions in mobile communications using multiple scattering," in *Proc. Gen. Assem. Int. Union of Radio Sci.*, Maastricht, The Netherlands, Aug. 2002.

[5] J. N. Laneman, D. N. C. Tse, and G. W. Wornell, "Cooperative diversity in wireless networks: Efficient protocols and outage behavior," *IEEE Transactions on Information Theory*, vol. 50, no. 12, pp. 3062–3080, Dec. 2004.

[6] D. Chizhik, G. J. Foschini, M. J. Gans, and R. A. Valenzuela, "Keyholes, correlations, and capacities of multielement transmit and receive antennas," *IEEE Transactions on Wireless Communications*, vol. 1, no. 2, pp. 361–368, Apr. 2002.

[7] K. Peppas, F. Lazarakis, A. Alexandridis, and K. Danagakis, "Cascaded generalized-K fading channel," *IET Communications*, vol. 4, no. 1, pp. 116–124, Jan. 2010.

[8] J. M. Romero-Jerez and A. J. Goldsmith, "Performance of multichannel reception with transmit antenna selection in arbitrarily distributed nakagami fading channels," *IEEE Transactions on Wireless Communications*, vol. 8, no. 4, pp. 2006–2013, Apr. 2009.

[9] N. C. Sagias, G. K. Karagiannidis, D. A. Zogas, P. T. Mathiopoulos, and G. S. Tombras, "Performance analysis of dual selection diversity in correlated weibull fading channels," *IEEE Transactions on Communications*, vol. 52, no. 7, pp. 1063–1067, July 2004.

[10] V. A. Aalo, T. Piboongungon, and G. P. Efthymoglou, "Another look at the performance of mrc schemes in Nakagami-m fading channels with arbitrary parameters," *IEEE Transactions on Communications*, vol. 53, no. 12, pp. 2002–2005, Dec. 2005.

[11] H.-C. Yang and M.-S. Alouini, "Generalized switch-and-examine combining (GSEC): A low-complexity combining scheme for diversity-rich environments," *IEEE Transactions on Communications*, vol. 52, no. 10, pp. 1711–1721, Oct. 2004.

[12] M. K. Simon and M.-S. Alouini, *Digital Communication over Fading Channels*, 2nd ed. Hoboken, New Jersey, USA: IEEE: John Wiley & Sons, Inc., 2005.

[13] H.-C. Yang, "New results on ordered statistics and analysis of minimum-selection generalized selection combining (GSC)," *IEEE Transactions on Wireless Communications*, vol. 5, no. 7, pp. 1876–1885, July 2006.

[14] Y.-C. Ko, M.-S. Alouini, and M. K. Simon, "Analysis and optimization of switched diversity systems," *IEEE Transactions on Vehicular Technology*, vol. 49, no. 5, pp. 1813–1831, Sep. 2000.

[15] H. Suzuki, "A statistical model of urban multipath propagation," *IEEE Transactions on Commun.*, vol. 25, pp. 673–680, 1977.

[16] F. Hansen and F. I. Meno, "Mobile fading-rayleigh and lognormal superimposed," *IEEE Transactions on Vehicular Technology*, vol. 26, pp. 332–335, Nov. 1977.

[17] F. Vatalaro and G. E. Corazza, "Probability of error and outage in a rice-lognormal channel for terrestrial and satellite personal communications," *IEEE Transactions on Commun.*, vol. 44, no. 8, pp. 921–924, Aug. 1996.

[18] P. S. Bithas, N. C. Sagias, P. T. Mathiopoulos, G. K. Karagiannidis, and A. A. Rontogiannis, "On the performance analysis of digital communications over generalized-K fading channels," *IEEE Communication Letters*, vol. 5, no. 10, pp. 353–355, May 2006.

[19] I. Trigui, A. Laourine, S. Affes, and A. Stephene, "On the performance of cascaded generalized-K fading channels," in *IEEE Global Telecommunications Conference (GLOBECOM 2009)*, Honolulu, Hawaii, US, Nov. 2009, pp. 1–5.

[20] A. Abdi and M. Kaveh, "On the utility of gamma pdf in modeling shadow fading (slow fading)," in *IEEE 49th Vehicular Technology Conference, 1999*, vol. 3, Houston, TX, US, Aug. 2002, pp. 2308–2312.

[21] D. J. Lewinsky, "Nonstationary probabilistic target and clutter scattering models," *IEEE Transactions on Antenna and Propagation*, vol. AP-31, no. 3, pp. 490–498, May 1983.

[22] P. M. Shankar, "Error rates in generalized shadowed fading channels," *Wireless Personal Communications*, vol. 28, no. 4, pp. 233–238, Feb. 2004.

[23] P. M. Kostic, "Analytical approach to performance analysis for channel subject to shadowing and fading," *IEE Proceedings on Communications*, vol. 152, no. 6, pp. 821–827, Dec. 2005.

[24] S. Al-Ahmadi and H. Yanikomeroglu, "On the approximation of the generalized-K distribution by a gamma distribution for modeling composite fading channels," *IEEE Transactions on Wireless Communications*, vol. 9, no. 2, pp. 706–713, Feb. 2010.

[25] A. Abdi and M. Kaveh, "K distribution: an appropriate substitute for rayleigh-lognormal distribution in fading-shadowing wireless channels," *Electronics Letters*, vol. 34, no. 9, pp. 851–852, Aug. 2002.

[26] "Wolfram functions," http://functions.wolfram.com/07.34.16.0003.01.

[27] I. S. Gradshteyn and I. M. Ryzhik, *Table of Integrals, Series and Products*. New York: Academic Press, 2000.

[28] M. D. Springer, *The Algebra of Random Variables*. John Wiley Sons, Inc., 1979.

[29] V. S. Adamchik and O. I. Marichev, "The algorithm for calculating integrals of hypergeometric type functions and its realization in reduce system," in *Proceedings of the International Conference/Symposium on Symbolic and Algebraic Computation*, 1990, pp. 212–224.

[30] V. Erceg, S. J. Fortune, J. Ling, A. Rustako, and R. Valenzuela, "Comparisons of a computer-based propagation prediction tool with experimental data collection in urban microcellular environments," *IEEE Journal on Selected Areas Commun.*, vol. 15, no. 4, pp. 677–684, May 1997.

[31] G. K. Karagiannidis, N. C. Sagias, and P. T. Mathiapoulos, "N* Nakagami: A novel stochastic model for cascaded fading channels," *IEEE Transactions on Commun.*, vol. 55, no. 8, pp. 1453–1458, Aug. 2007.

[32] N. C. Sagias and G. S. Tombras, "On the cascaded weibull fading channel model," *Journal of the Franklin Institute*, vol. 344, no. 1, pp. 1–11, Jan. 2007.

[33] D. Chizhik, G. J. Foschini, and R. A. Valenzuela, "Capacities of multielement transmit and receive antennas: Correlations and keyholes," *Electon. Lett.*, vol. 36, no. 13, pp. 1099–1100, June 2000.

[34] H. Shin and J. H. Lee, "Performance analysis of space-time block codes over keyhole nakagami-m fading channels," *IEEE Transactions on Vehicular Technology*, vol. 53, no. 2, pp. 351–362, Mar. 2004.

[35] G. K. Karagiannidis, T. A. Tsiftsis, and R. K. Mallik, "Bounds of multihop relayed communications in Nakagami fading," *IEEE Transactions on Communications*, vol. 54, no. 1, pp. 18–22, Jan. 2006.

[36] G. K. Karagiannidis, "Performance bounds of multihop wireless communications with blind relays over generalized fading channels," *IEEE Transactions on Wireless Commun.*, vol. 5, no. 3, pp. 498–503, Mar. 2006.

[37] G. K. Karagiannidi, T. A. Tsiftsis, and N. C. Sagias, "A closed-form upper-bound for the distribution of the weighted sum of rayleigh variates," *IEEE Commun. Lett.*, vol. 9, no. 7, pp. 589–591, July 2005.

[38] "Wolfram functions," http://functions.wolfram.com/07.34.21.0088.01.

[39] "Wolfram functions," http://functions.wolfram.com/07.34.03.0456.01.

[40] M.-S. Alouini and M. K. Simon, "Dual diversity over correlated log-normal fading channels," *IEEE Transactions on Communications*, vol. 50, pp. 1946–1959, 2002.

[41] M. H. Ismail and M. M. Matalgah, "Bit error rate of diversity M-phase-shift keying receivers in Weibull fading with cochannel interference," *IET Communications*, vol. 4, no. 1, pp. 13–25, 2010.

[42] P. M. Shankar, "Performance analysis of diversity combining algorithms in shadowed fading channels," *Wireless Personal Communications*, vol. 37, no. 1-2, pp. 61–72, Apr. 2006.

[43] P. S. Bithas, P. T. Mathiopoulos, and S. A. Kotsopoulos, "Diversity reception over generalized-K (K_G) fading channels," *IEEE Transactions on Wireless Communications*, vol. 6, no. 12, pp. 4238–4243, Dec. 2007.

[44] A. H. Wojnar, "Unknown bounds on performance in Nakagami channels," *IEEE Transactions on Communications*, vol. 34, no. 1, pp. 22–24, Jan. 1986.

[45] N. C. Sagias, D. A. Zogas, and G. K. Kariaginnidis, "Selection diversity receivers over nonidentical Weibull fading channels," *IEEE Transactions on Vehicular Technology*, vol. 54, no. 6, pp. 2146–2151, Nov. 2005.

[46] M. Abramowitz and I. A. Stegun, *Handbook of Mathematical Functions.* New York: Dover, 1972.

[47] M. Shah, "On generalization of some results and their applications," *Collectanea Mathematica*, vol. 24, no. 3, pp. 249–266, 1973.

[48] "Wolfram functions," http://functions.wolfram.com/07.34.21.0088.01.

[49] B. L. Sharma and R. F. A. Abiodun, "Generating function for generalized function of two variables," *Proceedings of the American Mathematical Society*, vol. 46, no. 1, pp. 69–72, Oct. 1974.

[50] A. M. Mathai and R. M. Saxena, *The H-Function with Applications in Statistics.* New York: Wiley Halsted, 1978.